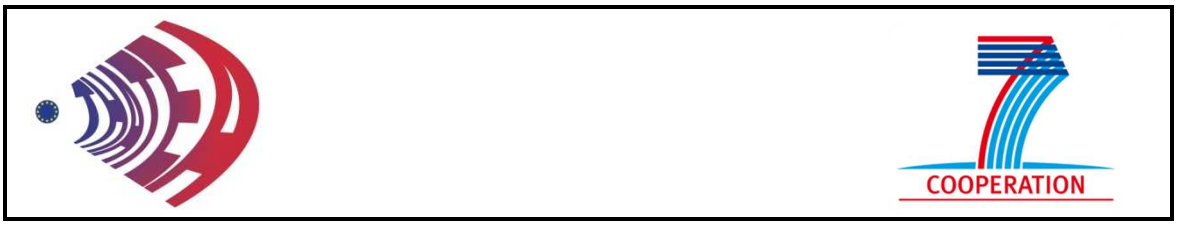

Grant Agreement no.: **226415**

Project acronym: THATEA

Project title:
THermoAcoustic Technology for Energy Applications

Instrument: Collaborative Project

Thematic Priority: **FP7-ENERGY-2008-FET**

FINAL REPORT

Date of preparation: 29.02.2012

Start date of project: 01.01.2009 Duration: 36 months

Project coordinator name: Simon Spoelstra
Project coordinator organisation: Energy research Centre of the Netherlands (ECN)

Contents

1. Executive summary

The objective of the THATEA (THermoAcoustic Technology for Energy Applications) project is to advance the basic scientific and technological knowledge in the field of thermoacoustics. The project will assess the feasibility of thermoacoustic applications to achieve conversion efficiencies of:

- Heat to acoustic power of 40% of the maximum theoretical Carnot efficiency;
- Acoustic power to heating/cooling of 40% of the maximum theoretical Carnot efficiency.

In addition, integrated systems should be investigated that couple the separate components, resulting in high overall system efficiency. This project is the first thermoacoustic initiative on a European level. The partnership consists of: two SME's (Aster, Hekyom), two research institutes (ECN, NRG) and three leading academic groups (CNRS, UNIMAN, UNIME).

A thermoacoustic system usually comprises an engine (producing acoustic power from heat), a heat pump (uses acoustic power to pump heat) and a resonator containing the engine and heat pump. The core of both engine and heat pump consist of a regenerator sandwiched between two heat exchangers. The main findings with respect to the different activities is summarized below.

Regenerator
Experiments were carried out to measure these heat transfer rate, pressure drop, and thermal conductivity for different regenerator materials. The conclusions that the friction factor results show good agreement with correlations from literature's and that the heat conduction through the regenerator material is overestimated when using the commonly used value of 0.15 as the thermal conductivity degradation factor.

Engines
Two different types of thermoacoustic engines have been constructed and tested. Both engines generate acoustic power from heat. The difference between the two engines concerns the driving temperature. The high-temperature engine uses heated air up to 800°C to simulate flue gasses from a burner, while the low-temperature engine uses heat up to 200°C as heat supply. The high-temperature engine achieved an efficiency of 41.5 % of the Carnot efficiency, thereby exceeding the target performance. The low-temperature engine showed an efficiency of 33 % of the Carnot efficiency with options identified fur further improvement.

Heat pumps
Two different types of thermoacoustic heat pumping devices have been constructed and tested. These two differ with respect to the temperature level on which they operate. One device pumps heat from 10°C to 80°C while the second acts as an refrigerator and pumps heat from -40°C to ambient temperature. The first device achieved 36 % of Carnot in the component testing but 40 % of Carnot as part of the integral system. The refrigerator showed a maximum performance of 33 % of Carnot. Noteworthy is that both components showed measured efficiencies much higher than previously measured worldwide.

Scaling
The scaling analysis shows that the linear approximation used for the design modelling of thermoacoustic systems functions very well. Heat losses by convection, conduction and radiation need careful attention since these are not adequately covered by the present modelling. In addition, more practical aspects with respect to scaling to larger powers were addressed. Most important issues are the construction of the heat exchangers, the manufacturability of the heat exchangers and possible more-dimensional effects.

Heat exchangers
Detailed measurements on heat exchange in oscillating flow conditions combined with numerical simulations have led to design rules (non-dimensional correlations) for thermoacoustic heat exchangers. These design rules relate to the length of the heat exchanger

and the fin spacing. The practical design of heat exchangers has to be improved to arrive at the situation where the heat transfer is optimal, combined with low costs of manufacturing.

Resonators
Two alternatives for the standard acoustic resonator were explored in this project. The first concept uses a traveling wave loop in combination with a multiple regenerator units. This concept runs at a low pressure amplitude (ensuring low losses) and has an inherent proper timing for each unit. The second concept replaces the acoustic resonator by a mechanical mass-spring system. The mechanical mass-spring could not be tested as an integral system but the component testing showed promising (low loss) results. The main conclusion is that the alignment of the cylinder in the piston is a very critical issue.

Non-linear phenomena
An experiment setup was used that is capable of measuring acoustic streaming inside the resonator. The measurement results were used to validate a Computational Fluid Dynamics (CFD) model. The qualitative agreement was reasonable but the quantitative agreement should be improved. CFD modeling proved to be a useful tool to study the time-independent phenomena that occur in oscillatory flow conditions. A thorough understanding of these phenomena is needed to identify countermeasures that stop streaming. This subject definitely requires further research.

Integral systems
Two integral systems have successfully been designed and taken into operation. Both systems show the required functionality. Both systems also show that the targeted performance is not reached. They reach about 60 % of the objective. While at the component level the efficiencies are 75 % or higher (even to 100 %) of the target, the multiplication of the efficiencies of the individual components leads to this overall result. The requirements for the optimal performance of the individual components do not always match with each other. For example, a high drive ratio leads to high useful powers compared to the heat losses and thus a high efficiency for an engine but at the same time a high drive ratio leads to high acoustic losses in the resonator. Several improvement options have been identified which should guide the way to a more efficient integral system.

Figure 1 *Overview of experimental facilities used within THATEA*

2. Summary description of project context and objectives.

Background
As stated in the EU-policy on energy, technology is vital in reaching all of our energy and climate change policy objectives: to reduce greenhouse gas emissions by 20% and ensure 20% of renewable energy sources in the EU energy mix; to reduce EU primary energy use by 20% by 2020. We need to accelerate the development and deployment of cost-effective, low carbon technologies. We need to lower the cost of clean energy and put EU industry at the forefront of the rapidly growing low carbon technology sector. In the long term, if we are to decarbonise our economy, new generations of technologies have to be developed through groundbreaking research.

The introduction of new, energy-efficient or renewable technologies is often hampered by the cost-effectiveness of these technologies. There is no economic incentive for the energy consumer to make use of alternative technologies that save energy or provide renewable energy. In order to reduce the energy demand for heat, cooling, power, and lighting, or provide this in a renewable way, a large variety of energy technologies is required. Each application is serviced by a given technology.

It would be very helpful if a generic energy technology existed that could provide the required energy function for different applications. This leads to an economy of scale and numbers for this technology which would accelerate its introduction.

Thermoacoustic (TA) energy conversion is such a generic cross-cutting energy technology that can be applied in a vast number of applications, requiring heating, cooling, or power

Technology concept
Thermoacoustic energy conversion can be used to convert heat to acoustic power (engine) and to use acoustic power to pump heat to higher temperature levels (heat pump). Acoustic power can also be converted with high efficiency to electricity and vice versa. Thermoacoustic energy conversion is a rather new technology. The systems use an environmentally friendly working medium (noble gas) in a Stirling-like cycle, and contain no moving parts. These properties will enable new applications which are not feasible today for technical or economic reasons. Although the dynamics and working principles of TA systems are quite complex and involve many disciplines such as acoustics, thermodynamics, fluid dynamics, heat transfer, structural mechanics, and electrical machines, the practical implementation is relatively simple. This offers great advantages with respect to the economic feasibility of this technology.

In principle, there is a large variety of applications possible for both TA engines and heat pumps, and their combinations. Generally speaking, most applications which involve heating, cooling, or electricity production can be addressed by the thermoacoustic systems. The specific situation, however, determines whether thermoacoustic systems have advantages over conventional systems. To be more specific, thermoacoustic systems can for example be applied as/for

- Heat pumps for domestic applications
- Heat pumps for upgrading industrial waste heat
- Conversion of solar irradiation to electricity
- Liquefaction and regasification of natural gas.
- Combined heat and power systems
- Tri-generation systems (power, heating, cooling)
- Solar driven cooling systems
- Conversion of geothermal heat to electricity

The working principles of thermoacoustic systems are quite complex. However, the practical implementations of these are relatively simple. This offers great advantages with respect to the economic feasibility of this technology. Other advantages include:

- No moving parts for the thermodynamic cycle, hence high reliability and a long life span;
- Environmentally friendly working medium (air, noble gas);
- The use of air or noble gas as a working medium offers a large temperature window because there are no phase transitions;
- Use of simple materials with no special requirements, which are commercially available in large quantities and therefore relatively cheap;
- Single technology can provide broad base for a large variety of applications.

Despite a significant scientific progress in developing thermoacoustic systems, the technology has still not reached a commercial stage. However this can change rapidly since TA technologies can offer many unique opportunities in many energy applications. This project is the first initiative on a European level, aiming to combine the efforts in the field of thermoacoustics in order to acquire a leadership position in this new, promising and innovative technology.

This project is dedicated to the exploration and the study of different conversion processes involved in TA systems and the potential they have for energy applications in the European industry. Because of the generic character of the thermoacoustic technology, the project is multi-disciplinary, involving many research and industrial partners from different application fields and different countries.

Objective

The objective of this project is to advance the science and technology behind the thermoacoustic energy conversion processes to such a level that would enable reaching conversion efficiencies at which the application of the technology becomes economically attractive. The quantitative objectives stated for this project are believed to ensure this.

These objectives will be achieved by carrying out the activities outlined in the proposed work plan. Issues that will be addressed in order to achieve improvements in performance are as follows:

- Research into the design of the acoustic network to ensure appropriate timing between pressure variation and gas displacement. This is critical in realising the Stirling cycle and therewith a high conversion efficiency;
- Studies into alternative regenerator materials and structures. The regenerator provides isothermal conditions by narrow passages which also are a major source of (viscous) dissipation. New regenerator structures such as parallel-plate or parallel-tube regenerator instead of the screen-bed regenerator used conventionally will be investigated. Using a regenerator with a regular structure (dimensions in the order of 100 μm) would have lower viscous losses while still providing the necessary regenerative heat exchange;
- Investigations of heat exchangers as critical system components having to provide high heat transfer rates within physically constricted spaces. Large temperature losses between heat exchangers and regenerators will immediately results in lower system performance. The heat exchangers have to be optimised for oscillating flow;
- Non-linear effects occurring in TA systems at high pressure amplitudes. There are several types of these effects and these are yet not fully understood. Moreover, they have a negative effect on the performance of the system. The understanding and suppression of these non-linear effects will therefore be important in improving system performance.
- Optimisation of the geometry of the acoustic resonator. This will minimize the thermo-viscous losses and hence result in a better performance. Alternative resonator concepts are also feasible, for example the use of mechanical resonators or pure travelling wave resonators.

- Studies of integrated systems. Thermoacoustic engines and heat pumps comprise of a range of different components. The coupling of these components resulting in an efficient system is not trivial and systems integration issues will need to be carefully addressed.

The table below summarises the envisaged scientific and technological progress beyond the current state-of-the-art in fulfilling the objectives of this project. For different research themes, the present state-of-the art is given in the worldwide context. In addition, the targets for the THATEA project are indicated. These targets not only relate to quantitative objectives but also to a range of technical options that will be pursued in individual research areas. As can be seen from the table, the objectives of the THATEA project are very ambitious.

Table 1 *Targeted progress compared to the State-of-the-art*

Issue	**State-of-the-art Worldwide**	**Target for THATEA**
Regenerators	Random stacking of stainless steel screens	uniform flow channels such as parallel plates or honeycombs sections
Heat supply	Electrical heaters	Heat exchangers for - Gas burner - Low-temperature heat
Heat exchangers (HX)	Shell and tube or finned tube HX's designed using steady flow correlations	Optimised HX's for the oscillatory flow conditions
Resonator	$\lambda/2$ and $\lambda/4$ type acoustic resonators	Improved acoustic resonators and mechanical resonators
Engine efficiency	LANL (USA) 40 % of Carnot	40 % of Carnot
Heat pump efficiency	PSU (USA) 19 % of Carnot	40 % of Carnot
Integral system for cooling purposes	LANL (USA) 1.2 % of Carnot Nagoya (Japan) 0.7 % of Carnot CAS (China) 2.8 % of Carnot	15 % of Carnot[1]
Integral system for heating purposes	None existing	40% of Carnot[2]

[1] Cooler (-40ºC, 20ºC) driven by a low temperature engine (120ºC, 20ºC) gives a Carnot efficiency for integral system of 0.98.
[2] Heat pump (10ºC, 80ºC) driven by high temperature engine (600ºC, 80ºC) gives a Carnot efficiency for integral system of 3.4.

3. Description of the main S&T results/foregrounds

A thermoacoustic system usually comprises an engine (producing acoustic power from heat), a heat pump (uses acoustic power to pump heat) and a resonator containing the engine and heat pump. The core of both engine and heat pump consist of a regenerator sandwiched between two heat exchangers. The activities in this project are divided into 6 Work packages (excluding project management). Each work package addresses a component or phenomenon within thermoacoustic systems. Research is carried out on thermoacoustic engines, on heat pump/refrigerators, on resonators, on thermoacoustic heat exchangers, on regenerator material, and on non-linear phenomena occurring in these systems. The picture below shows a schematic thermoacoustic system and (some of) the experimental setups that have been built within this project to study components within this system.

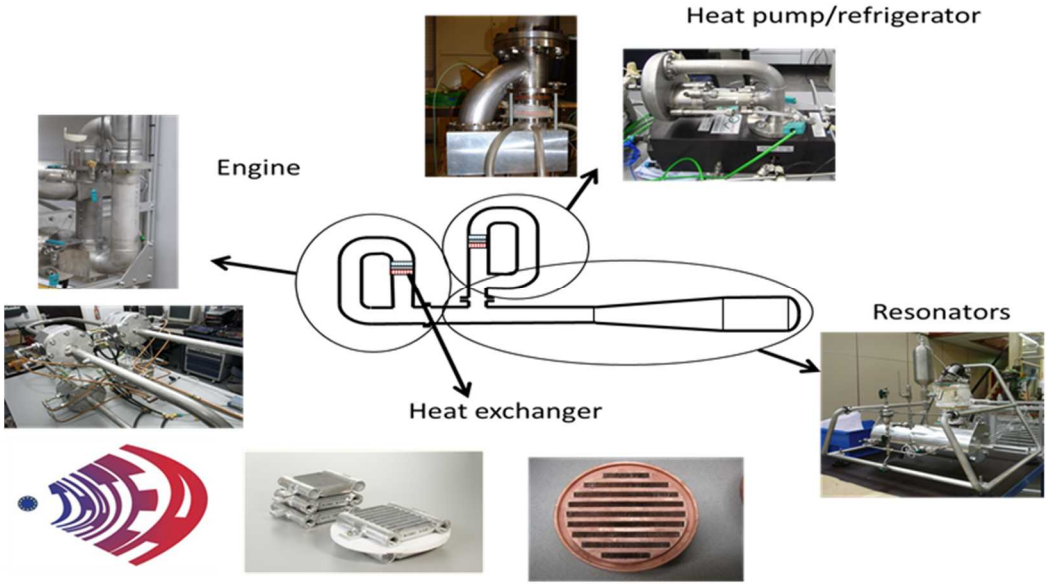

The following sections more or less follow the structure of the work packages. The work on the regenerator, which took place both for engines and heat pumps is addressed separately, as is a study on scaling of thermoacoustic systems.

3.1 Regenerator

The objective of this activity is to develop experimental facilities and experimental methodologies for the characterization of regenerator samples with different geometries, characteristic dimensions and made out of different materials. The results are to be expressed using dimensionless parameters, to formulate the regenerator design rules..

An ideal regenerator has perfect thermal contact with the gas (thermal time constant = 0), has a low pressure drop and a low axial thermal conductivity. Accordingly, three types of tests are used to characterize regenerators: (1) thermal time constant ($\omega\tau$) measurements; (2) flow resistance measurements; and (3) thermal conductivity measurements.

Thermal time constant measurements
The setup used is shown in Figure 2. The mean pressure can be varied from 1 to 40 bar. The working gas is helium. The excitation frequency of the acoustic driver can be varied from 20 to 120 Hz. The valves that are visible in Figure 2 are used to obtain the right phase relationship between pressure and velocity at the regenerator.

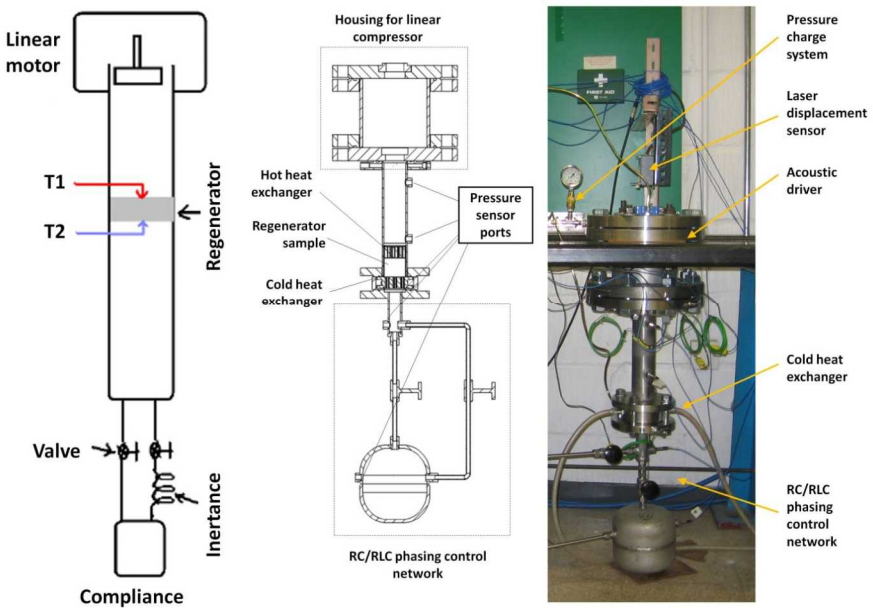

Figure 2 *Experimental apparatus for determining the time constant of the regenerator material*

Different samples of regenerator materials were tested. The commonly used woven metal screens varied from mesh number 30 to 200 (meshes/inch). In addition, a needle array regenerator was tested. The results clearly show that the values of $\omega\tau$ strongly depend on the velocity, see Figure 3. A higher velocity leads to a lower $\omega\tau$ in the regenerator. It can also be found that the length of the sample affects the measured $\omega\tau$ values. A long length leads to a higher value of $\omega\tau$ for the same test conditions.

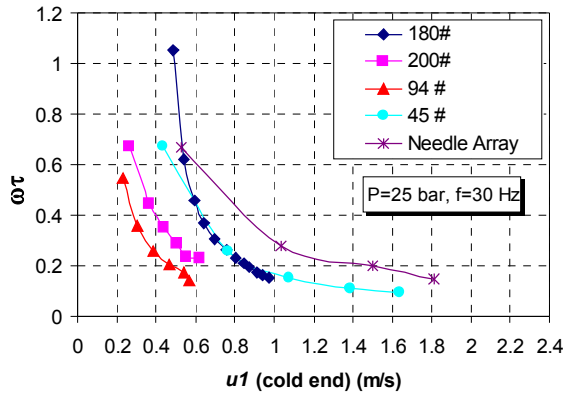

Figure 3 *ωτ experimental results*

Flow resistance measurements

The friction factor in the regenerator can be determined by measuring the pressure drop and the average velocity at which the fluid is passing through the regenerator. Historical data for porous media are available from measurements of Kays and London. Swift & Ward fitted these data into correlations, that are often used in thermoacoustic design codes. The experimental apparatus comprises of a 3 m long PVC pipe connected to the high pressure air supply via an adjustable valve that controls the air flow rate, shown in Figure 4.

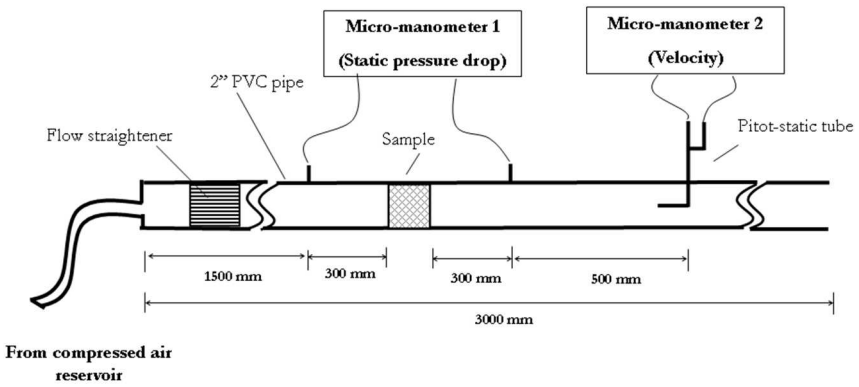

Figure 4 *Schematic diagram of the flow resistance measurement rig*

The obtained correlations are summarized in Table 2 and compared to Swift & Ward.

Table 2 Correlations between friction factor and Reynolds number for the regenerators tested

Regenerator Sample	Measured Correlation	Swift and Ward Correlation
45 #	$f_{F\_meas} = \frac{40.2}{R_e} + 0.16$	$f_F = \frac{34.2}{R_e} + 0.48$
180 #	$f_{F\_meas} = \frac{38.7}{R_e} - 0.37$	$f_F = \frac{34.2}{R_e} + 0.48$
200 #	$f_{F\_meas} = \frac{45.1}{R_e} - 0.66$	$f_F = \frac{39.7}{R_e} + 0.37$
94 #	$f_{F\_meas} = \frac{54.5}{R_e} - 0.2$	$f_F = \frac{38.2}{R_e} + 0.38$
30 #	$f_{F\_meas} = \frac{46.8}{R_e} + 0.27$	$f_F = \frac{35.4}{R_e} + 0.41$
Needle-array	$f_{F\_meas} = \frac{14.03}{R_e}$	$f_F = \frac{16}{R_e}$

Thermal conductivity measurements

The thermal conductivity of the regenerator specimens is measured by passing a constant heat flux through a known sample and an unknown sample and comparing the respective thermal gradients, which are inversely proportional to the samples' thermal conductivities. The setup is shown in Figure 5

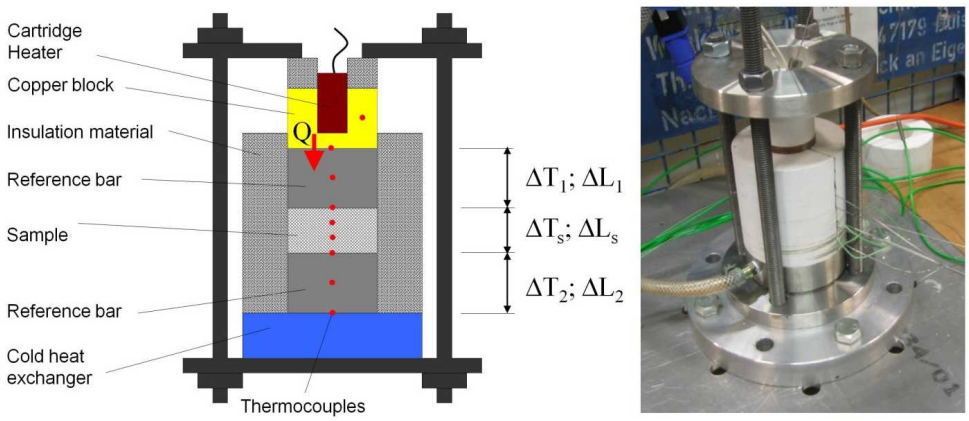

Figure 5 *Illustration of the setup for thermal conductivity measurements*

For regenerator materials such as mesh screens, the thermal conduction can be represented by a thermal conductivity degradation factor (TCDF). It is defined as the ratio of actual heat conduction to the heat conduction where the sample is assumed to be a solid rod of the cross-sectional area equal to the sample area multiplied by the fraction of the solid material in the mesh screen (1-ϕ). In this report, the experimental results are expressed in terms of the TCDF.

Figure 6 shows the measured TCDF when the temperature difference between the two ends of the sample varies. The samples are tested with a length around 6 mm. The measured TCDF depends on the dimensions of the samples. The general trend seems to be that higher mesh numbers lead to higher TCDF. However, there is one exception: the values for the sample with mesh number 30 are higher than those for the sample with mesh number 45. The reason for this behaviour is unclear.

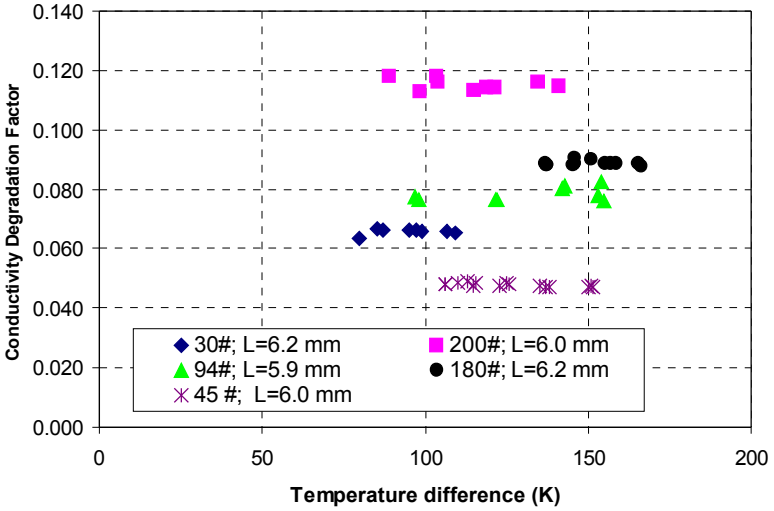

Figure 6 *Results of thermal conductivity measurements expressed in terms of TCDF*

Conclusions

- The results clearly show that the dimensionless parameter $\omega\tau$ strongly depends on velocity. A higher velocity leads to a lower $\omega\tau$.
- For given working conditions, a lower $\omega\tau$ corresponds to a better performance.
- The friction factor results show good agreement with Swift and Ward's correlation (used often in system codes) for low values of the Reynolds numbers. However, for relatively high Reynolds numbers, there is an apparent discrepancy between the measured results and the Swift and Ward's correlation, which is larger when the mesh number is lower.
- For the needle array, the friction factor results agree well with the theoretical ones.
- The measured thermal conductivity degradation factor depends on the mesh number. A higher mesh number leads to a higher thermal conductivity degradation factor.
- For all of the tested samples, the measured thermal conductivity degradation factors are less than 0.15 as proposed by others and is widely used in for example Delta EC.
- According to the results obtained in this report, the heat conduction through the regenerator material seems to be overestimated when using 0.15 as the higher thermal conductivity degradation factor in Delta EC for mesh screens with lower mesh numbers.

3.2 Thermoacoustic engines

The objective of this activity is to design, build, and test two thermoacoustic engines, for two different applications. One engine will be driven by high-temperature heat (burner, etc.), and a second one driven by low-temperature heat (< 200°C). The goal is to demonstrate an efficiency of 40 % of the maximal attainable Carnot efficiency for both types of engines.

3.2.1 High-temperature engine

The high-temperature traveling-wave thermoacoustic engine uses hot air (to simulate flue gases from a burner) as a heat source. Helium gas at an average pressure of 40 bar is used as the working medium at an operating frequency of 120 Hz. The thermoacoustic-Stirling engine consists mainly of three parts: a thermodynamic part consisting of a regenerator, two heat exchangers, and a thermal buffer tube; an acoustic network consisting of an acoustic compliance and an inertance; and a ¼-wavelength resonator with an acoustic load. A picture of the high temperature engine is shown in Figure 7.

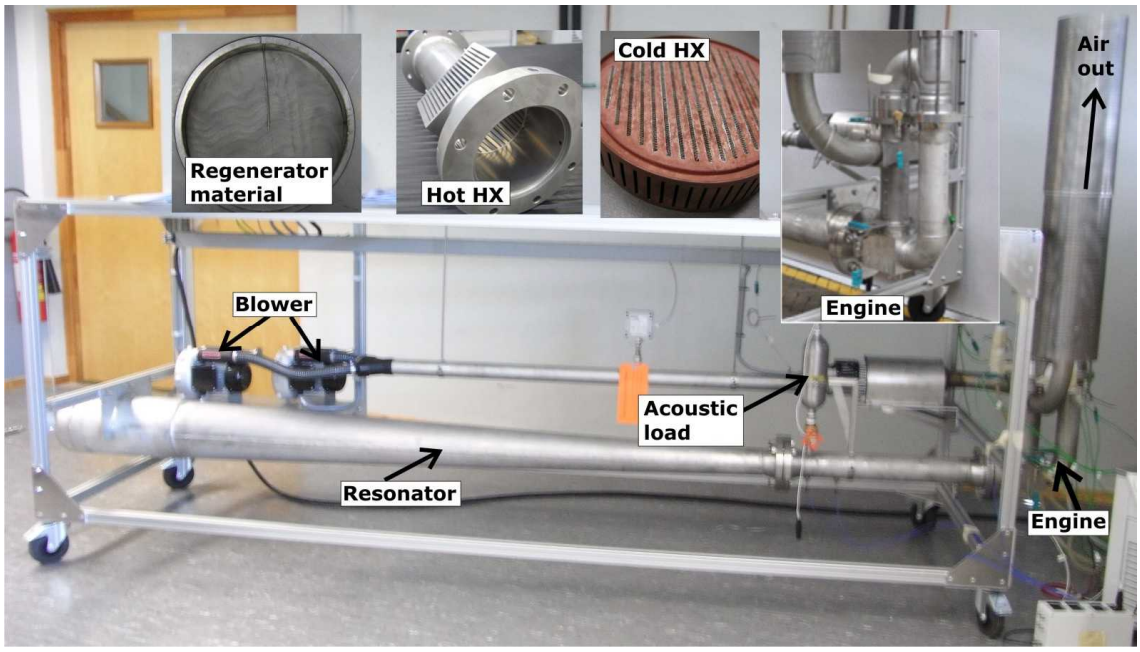

Figure 7 *Photograph of the high temperature thermoacoustic engine*

The test rig is equipped with numerous sensors to measure temperature, flow, dynamic and static pressure. The acoustic power produced by the engine at the resonator junction is the sum of the acoustic power dissipated in the whole resonator and that dissipated in the load. The performance of the engine is given by the acoustic power produced by the engine divided by the thermal power supplied by the hot air. This performance is compared to the theoretical Carnot efficiency to obtain the relative efficiency which was defined as target for this project.

The performance of the engine as a function of the temperature of the hot air is given in Figure 8. The performance increases as function of the hot air temperature and as function of the drive ratio. The engine achieves a performance of 41.5 % at a drive ratio of 6 % and a hot air temperature of 620°C, therewith exceeding the target for this engine. This relatively good performance is obtained in spite of a considerable heat leakage (about 30 % of the heat input). through the thermal buffer tube. An improvement of the performance might be expected by suppressing this heat leak caused by streaming.

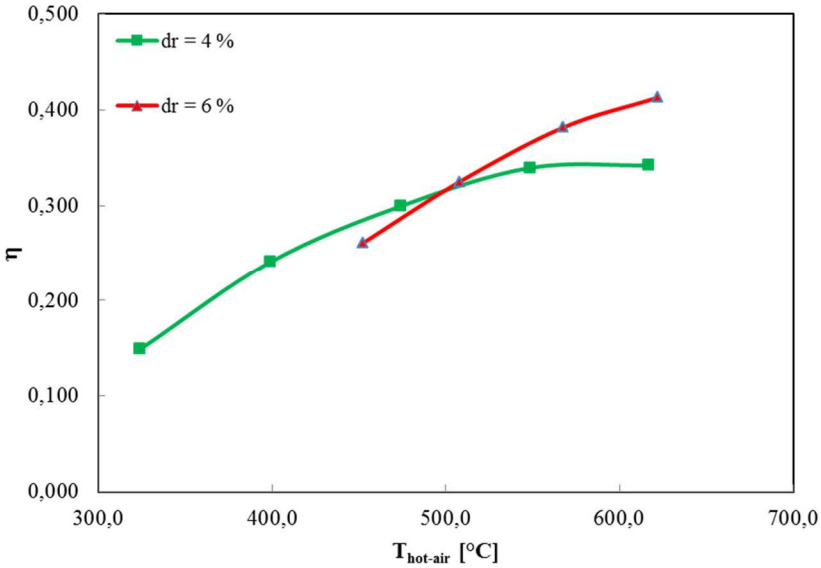

Figure 8 *Measured performance of the high-temperature engine relative to Carnot as a function of the hot air temperature for two drive ratios*

Conclusions

The high-temperature engine shows an efficiency above the target of 40% of the Carnot efficiency. The performance increases with increasing drive ratio which require a high heat input at the hot heat exchanger. The required heat transfer at this (gas-gas) heat exchanger puts high requirements on the quality of this heat exchanger. The engine also suffers from relatively large heat losses.

3.2.2 Low-temperature multi-stage engine

At declining temperatures thermoacoustic engines become increasingly more sensitive to imperfections like heat exchanger temperature drop and to acoustic impedance matching and dissipation. Thermoacoustic power gain is proportional with the operating temperature consequently leading to less gain at lower temperatures. One way to overcome this problem, and to allow for efficient operation at declining temperatures (< 200°C), is to increase the (thermo)acoustic power gain by using multiple regenerator units.

The initial low-temperature engine is build up from four identical regenerator units which are connected acoustically in series by near traveling wave loop sections. The mutual distance between the regenerator units is a quarter wavelength. The construction and final test set-up are shown in Figure 9.

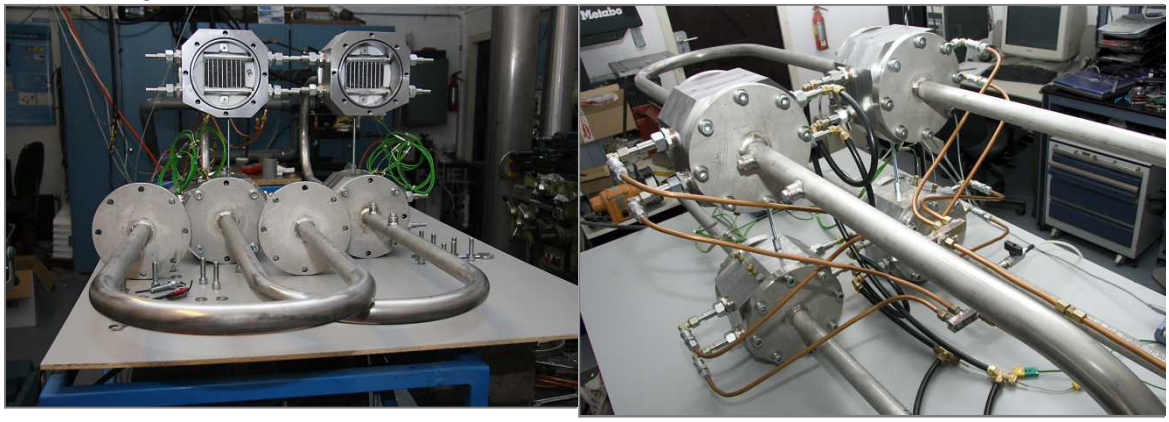

Figure 9 *Construction and final test set-up of the low temperature engine*

Low cost aluminum brazed louvered fin heat exchangers are used to supply and remove heat from the thermoacoustic process in the regenerator. Instrumentation is provided to measure regenerator and water temperatures and acoustic power at different locations along the loop.

Measurements with an unloaded engine are performed for both argon (29 Hz) and helium (90 Hz) as working gas at various mean pressures. More specific, the engine was characterized based on starting temperatures and the increase in loop power depending on the temperature difference across the regenerator. The result for various mean pressures is shown in Figure 10.

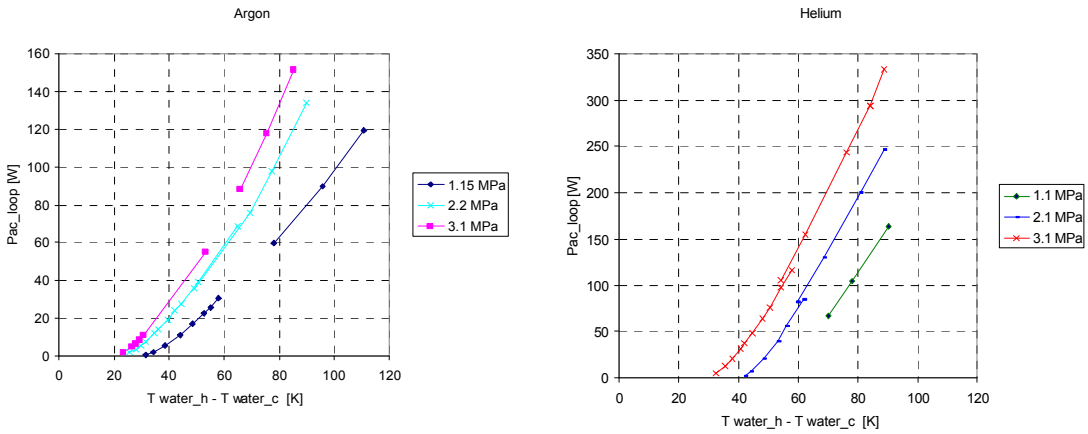

Figure 10 *Measured loop power versus temperature difference between the high and low temperature water circuits for both argon and helium*

A very low onset temperature difference of only 22 K is obtained for argon at a mean pressure of 3.1 MPa This is the lowest onset temperature reported so far for a thermoacoustic engine but more important, it is an essential condition for efficient operation of the project low temperature integral system. The onset temperature for helium is only slightly higher with 31 K because the regenerator initially was optimized for 4 MPa and 120 Hz.

A variable acoustic load was added to be able to calculate the real engine output power. The results for this test are summarized in Table 3.

Table 3 *Measurement on the 3 stage engine loaded with cooler*

Measured values	**Notes**
P_0 = 3.1 Mpa	
$T_{C\_water\ in}$ = 40.4 °C	
$T_{H\_water\ in}$ = 164 °C	
P_{ac_loop} = 169 W	measured at input #1
P_{ac_out} = 90.8 W	power dissipated in #1 + dummy load
Q_c = 888 W	
Eff_T = 9.3%	Thermal efficiency = P_{ac_out} / (Q_C + P_{ac_out})
Eff_{ex} = 33%	exergetic efficiency is relative to the Carnot factor

Table 3 indicates that the exergetic efficiency of the low temperature engine should be further improved up to at least 40%. There are a few options to reach this target which will be implemented in the integral system.

Conclusions
The conclusion of the testing of the low-temperature engine shows an efficiency slightly below the target of 40% of the Carnot efficiency. The engine suffers little from heat losses and runs at a low drive ratio. Heat exchangers is this system are very critical since the driving temperatures are low and temperature losses should be avoided as much as possible.

3.3 Thermoacoustic heat pumps

The objective of this work package is to design, build, and test a thermoacoustic heat pump and a thermoacoustic refrigerator to enable two different applications. The heat pump will take heat at 10°C and upgrade it at 80°C. The refrigerator will deliver its cooling power at –40°C. The goal is to demonstrate an efficiency of 40 % of the Carnot efficiency for both types of application.

3.3.1 Heat pump 10°C to 80°C

To test the heat pump separately, an experimental setup is used where a linear motor drives a heat pump. Figure 11 shows an overview of the experimental bench. The heat pump, driven by the linear motor (the black box) is shown separately in more detail.

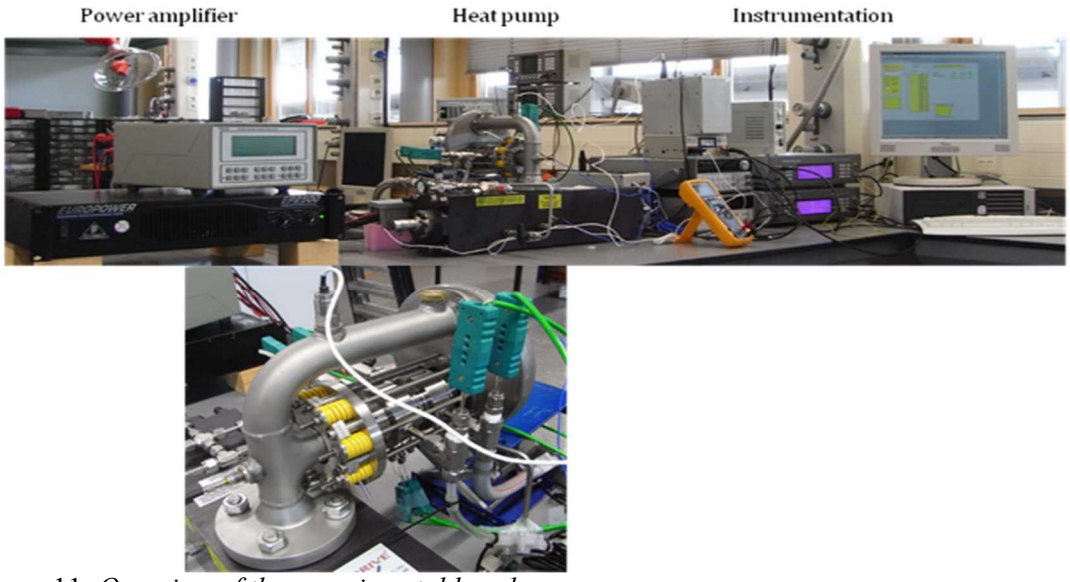

Figure 11 *Overview of the experimental bench*

The setup is equipped with multiple pressure, temperature, and flow sensors. The performance of the heat pump is determined by measuring the acoustic power input to the heat pump and the thermal power input/output to/from the heat exchangers. Experiments were performed with the water inlet of the cold heat exchanger fixed at 10°C for all the measurements. The temperature of the water of the hot heat exchanger was varied from 60°C to 80°C. The frequency of operation is 98 Hz which is the resonance frequency of the linear motor coupled to the heat pump. The filling pressure is about 30 bar helium. Figure 12 shows the performance of the heat pump as a function of drive ratio. The maximum performance reached 36 % of Carnot for a drive ratio of 3 %.

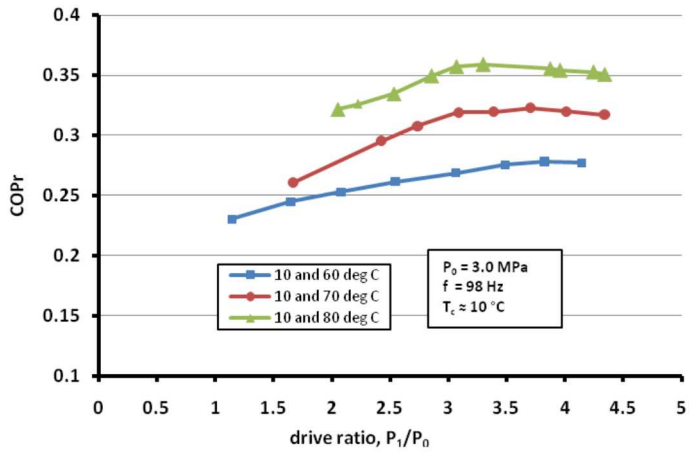

Figure 12 *Measured COP relative to Carnot as function of the drive ratio for three different hot temperatures. The cold temperature is fixed at 10°C*

The experimental data are analysed and compared to the DeltaEC model. The measured and calculated acoustic power and output heat are shown in Figure 13. The measured heat is in good agreement with that calculated by the model. However, the measured acoustic power is slightly higher than the calculated values. This additional acoustic power used by the heat pump could be due to losses in the thermal buffer tube which are not well modelled. This argument is also supported by the fact that the use of flow straighteners in the thermal buffer tube has improved the performance of the heat pump.

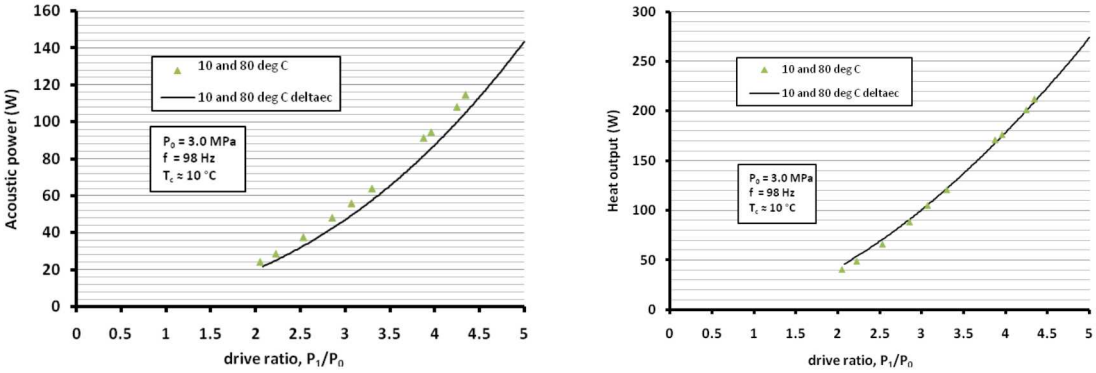

Figure 13 *Acoustic power at the pistons (left) and heat output at hot heat exchanger (right)for several drive ratios. The calculated quantities are plotted with a solid line*

Although the targeted efficiency of 40 % of Carnot was not reached in the heat pump, the performance came with 36 % close to this target. In order to improve the performance for the heat pump, the following modifications are recommended:

- Redesign the feedback inertance to provide a more optimal (about zero at the centre of the regenerator) phase difference between pressure and volume velocity.
- Engineer a more gradual branch between the feedback inertance and the thermodynamic section (the current design has a T-branch)

3.3.2 Refrigerator

The refrigerator was driven by a thermoacoustic prime mover. The experiments were carried out with a maximum helium gas pressure of about 38 bars. The refrigerator and the prime mover operated at about 123 Hz. Figure 14 pictures the refrigerator in testing operation without thermal insulation.

Instrumentation was set up within the heat exchangers to assess the thermal fluxes and evaluate the efficiency of the refrigerator. Several thermocouples are used to measure the temperature on the wall of the refrigerator components. The acoustic field inside of refrigerator is evaluated by use of four dynamic pressure sensors.

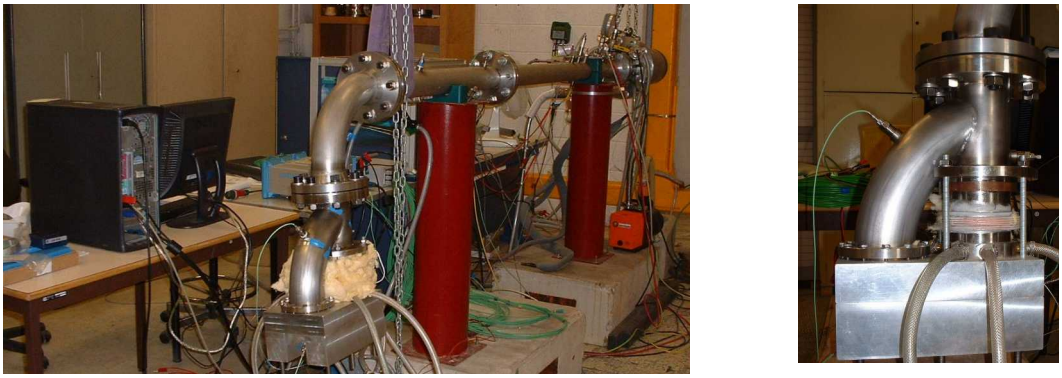

Figure 14 *Overview of the refrigerator driven by the thermoacoustic prime mover*

The original design was modified with different designs of the thermal buffer tube to reduce thermal convection caused by acoustic streaming. Figure 15 exhibits the measured coefficient of performance of the refrigerator relative to Carnot's performance as a function of the cold power and for three buffers. The aftercooler temperature (hot temperature) was fixed at 20 ºC by use of circulating water; the cold temperature was fixed at -40°C adjusting the electrical power of the heater.

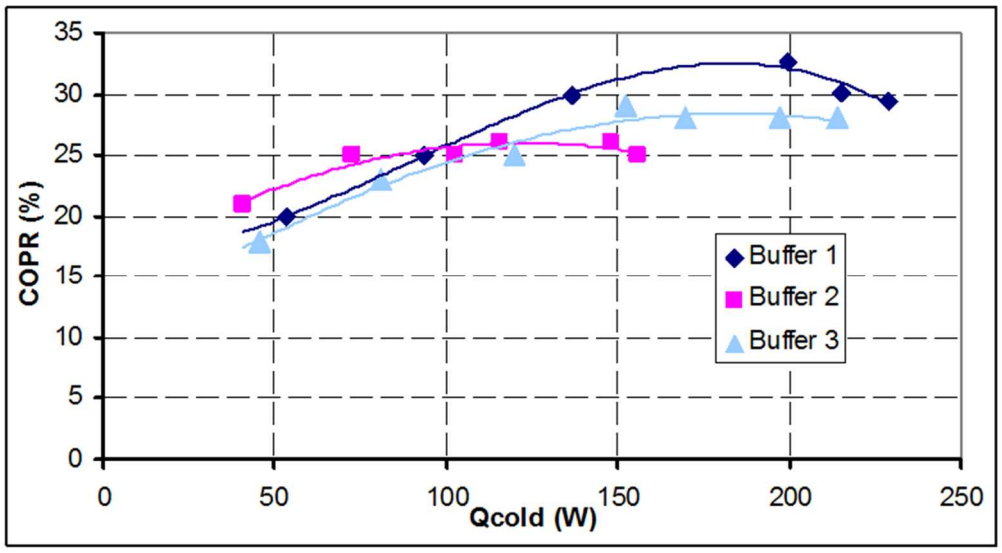

Figure 15 *COPR as a function of cold power for a cold heat exchanger temperature of 233K*

Besides efficiency the cooling power is also an important parameter. This cooling power can be influenced by modifying the feedback inertance. Inserts were placed inside the feedback inertance to assess the changes of the operating points of the refrigerator. Figure 16 shows the changes of the cooling power induced by the three inserts and the corresponding COP_R. This shows that more cooling power can be obtained at the expense of a lower efficiency.

.

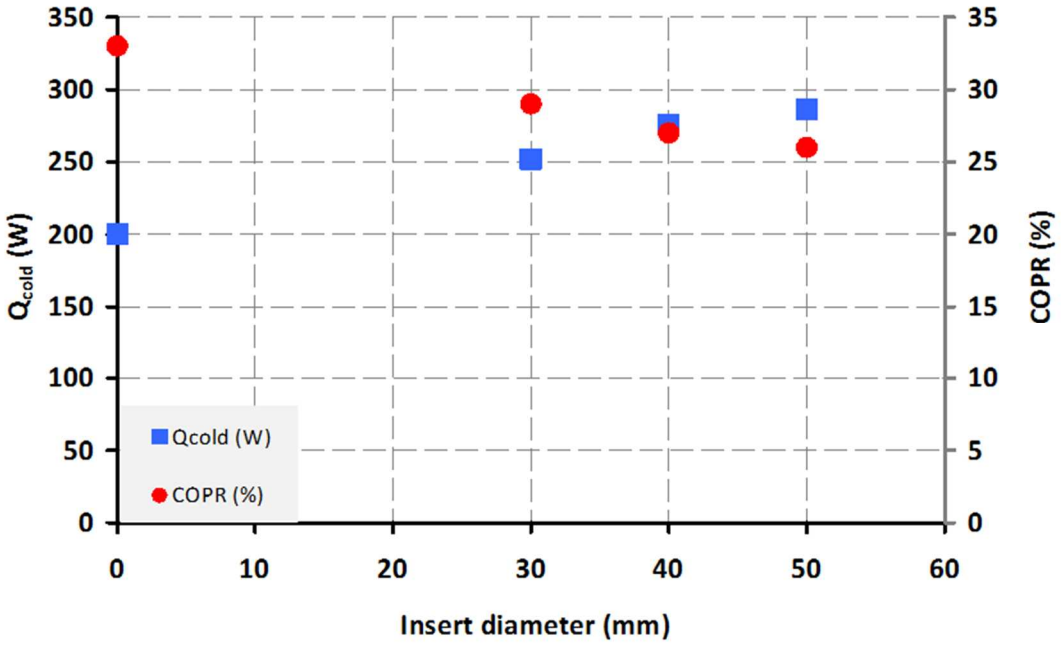

Figure 16 *Evolution of Qcold and COPR as a function of the inductance insert diameter for a cold heat exchanger temperature of 233K*

Conclusions
The refrigerator showed a maximum performance of 33 % of Carnot. Careful design of the buffer tube and the feedback inertance are necessary to achieve high efficiencies.

3.4 Scaling

Two types of scaling analysis have been carried out. The first study verifies experimentally the non-dimensional scaling rules for thermoacoustic systems. The second study looks at the practical aspects when scaling up thermoacoustic systems.

Non-dimensional scaling rules
The high-temperature traveling-wave thermoacoustic engine is used to verify the scaling rules for thermoacoustic systems. The scaling rule applied is the so-called pressure-gas scaling in which a low pressure, heavy gas system is compared to a high pressure, light gas system. In this case a 15 bar argon system is compared to a 40 bar helium system. The scaling rules dictate that these systems are acoustically identical but have a power ratio of 9 (He/Ar)

Figure 17 shows the results of the experiments. The powers and efficiency are plotted as function of the temperature of the hot air. The heat leak through the regenerator (static measurements) is subtracted from the experimental results as it doesn't follow the scaling rules. Figure 17 shows that the powers for the helium system are about a factor 9 larger than the thermal power in the argon system and that the efficiencies are comparable for both systems. This is in excellent agreement with the theory. This results indicate that the scaling rules works and that they can be used for the scaling up of thermoacoustic systems.

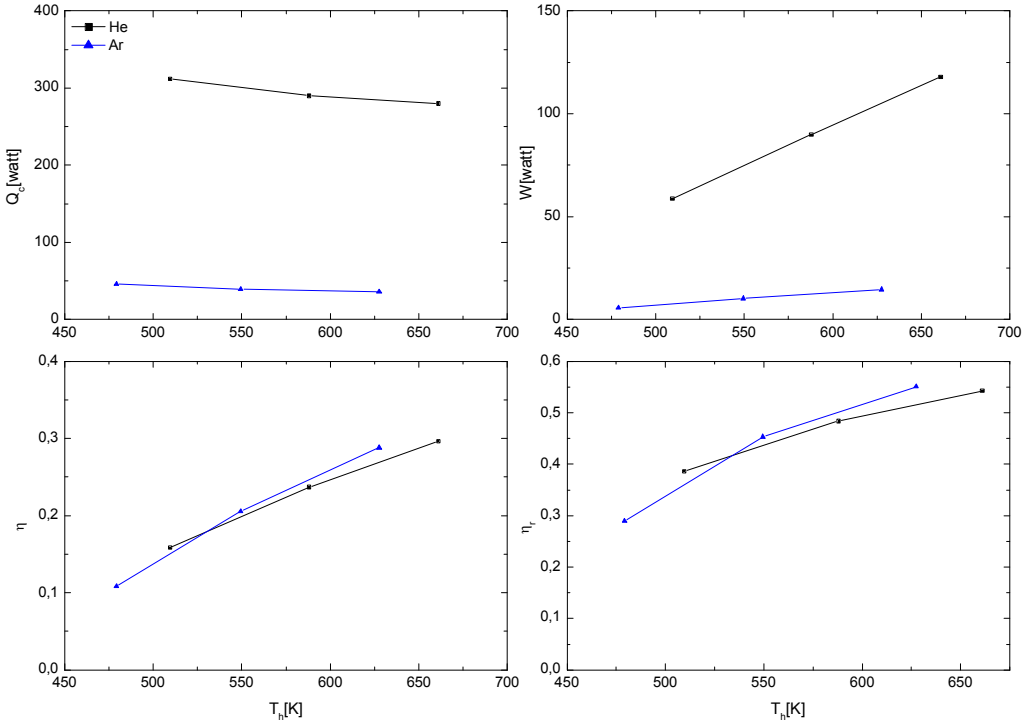

Figure 17 *Corrected measured thermal power at the ambient side for the torus engine filled with 15 bar Argon and with 40 bar Helium at a drive ratio of 3.5 %*

The scaling analysis shows that the linear approximation used for the design modelling of thermoacoustic systems functions very well. Heat losses by convection, conduction and radiation need careful attention since these are not adequately covered by the present modelling.

Practical aspects
A scaling study has been performed to analyse the consequences of increasing the power of thermoacoustic systems on efficiency, manufacturability, and possible new phenomena. The drive ratio, frequency, mean pressure and the diameter of the system are used as independent parameters to increase the power of the system.

The effect on efficiency has been studied by evaluating the thermal losses from the system in comparison with the useful acoustic power. All analyses show that the ratio between thermal losses and acoustic power decreases with increasing acoustic power. This can easily be understood since the acoustic power scales with the square of the diameter while the thermal losses scale linearly. High frequency would also be beneficial since this leads to compact systems with small surface areas. However, too high frequencies will lead to manufacturing problems with the heat exchangers.

With increasing power levels, the diameter of the resonator will increase, giving a certain frequency. The leads to heavier systems. This can be compensated by a higher frequency, but this will lead to problems with the heat exchangers, as explained above.

Heat exchangers are a crucial component in a thermoacoustic system. The length is determined by the frequency and drive ratio. The higher the drive ratio, the longer the heat exchanger. The higher the frequency, the shorter the heat exchanger. A low frequency and a high drive ratio enable a long heat exchanger, therewith increasing the surface area for heat transfer.

As the power increases, it becomes more difficult to realise the feedback loop, due to the limited bend radius that can be realised, giving a pipe diameter. A lower frequency is helpful in increasing the length of the feedback loop, making is easier to produce. Another option would be to create multiple smaller parallel feedback loops.

There are a couple of phenomena that could occur at large scale systems. Thermoacoustic systems are designed as one-dimensional systems. This means that the diameter should be small compared to the wavelength. The requirement should be carefully checked when the diameter is increased for a larger power system. Secondly, streaming within a regenerator could occur at larger diameters and lead to lower efficiencies. A third phenomenon is natural convection. This hardly occurs at small-scale systems but will have an increasing influence at larger diameters. Design measures should be taken to account for this.

3.5 Heat exchangers

The overall objective of this work package is to develop the understanding of heat transfer under oscillatory flow conditions by modelling and experiments and to use this knowledge to optimise heat exchangers for thermoacoustic systems. The research effort is focused on three main areas of activities: fundamental research into the heat transfer mechanisms within heat exchangers, developing Computational Fluid Dynamics modelling capabilities based on fundamental findings, and the design work for practical heat exchangers that are optimised for performance and are economically affordable.

3.5.1 Experimental research

Two types of experimental studies are carried out: investigation of thermal-fluid processes within heat exchangers on the micro-scale of an individual channel (local/time resolved), and heat transfer performance measurements in macro-scale arrangements to obtain "lumped" quantities.

Study of heat exchangers in micro-scale

Fin-type heat exchangers are chosen in this study of heat transfer process. The flow and temperature fields are measured, by employing Particle Image Velocimetry (PIV) and Planar Laser Induced Fluorescence (PLIF), in a channel between fins of "hot" and "cold" heat exchangers and in the vicinity of the two heat exchangers. The oscillatory flow is induced by an acoustic wave (13.1 Hz), maintained by a subwoofer type loudspeaker in a resonator. A schematic drawing of the flow rig and a close-up view of the test section with the LIF system setup are shown in Figure 18.

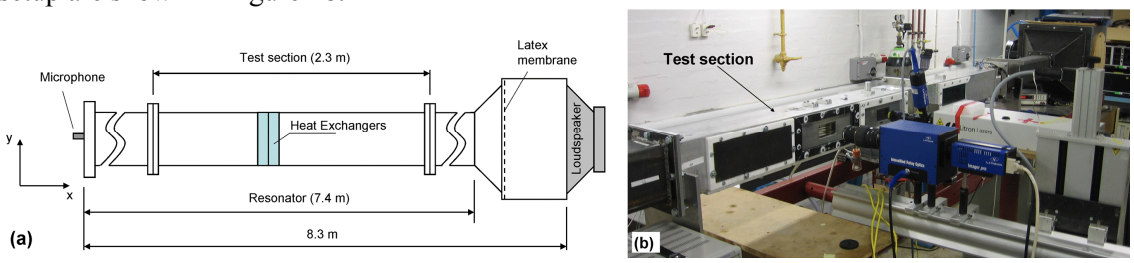

Figure 18 *Schematic of the experimental setup (a) and a close-up view of the test section (b)*

Two pairs of large-scale hot and cold heat exchangers have been fabricated. Figure 19 shows sample velocity fields in the channel of the first set of heat exchangers at four selected phases, at the velocity amplitude 1.3m/s and the temperature difference 0°C. Such data were mainly used to validate the CFD results for the heat exchanger channel.

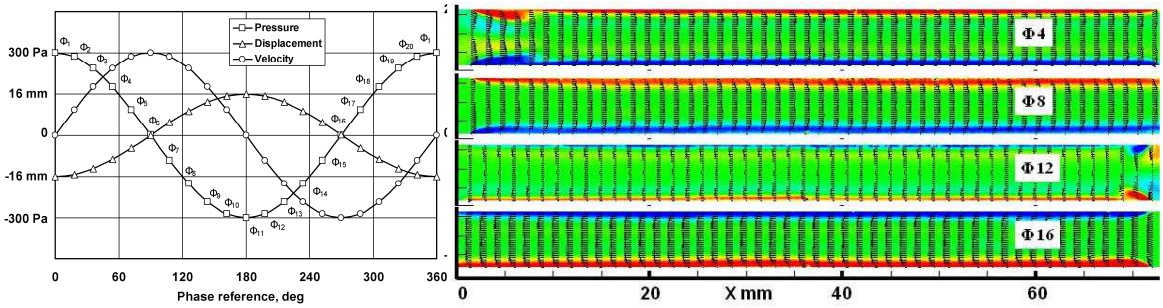

Figure 19 *(a) Relative phasing between pressure, velocity and displacement (in this example: displacement amplitude is 16 mm). (b) Sample velocity fields obtained at velocity amplitude 1.3 m/s and temperature difference of 0°C*

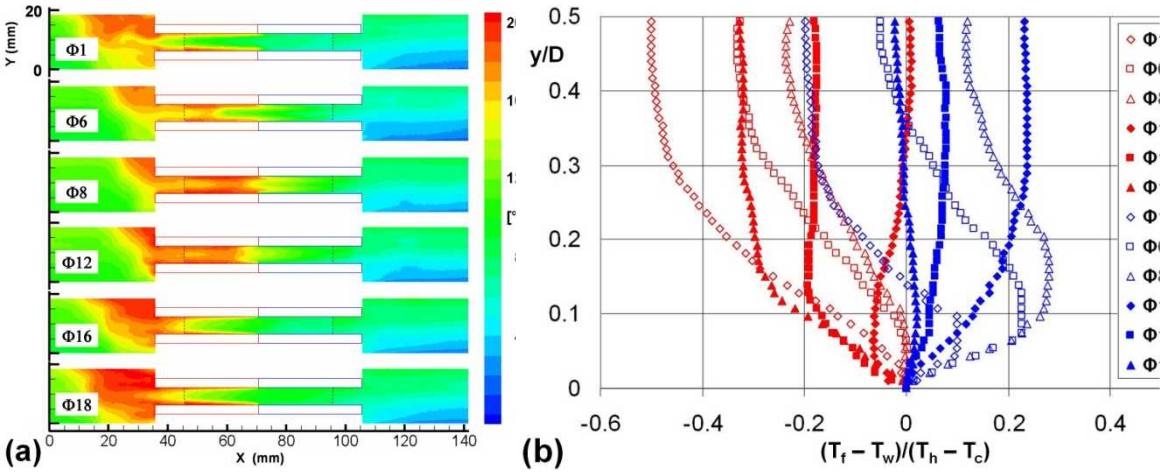

Figure 20 *(a) Temperature fields for six selected phases at the velocity amplitude of 1.30 m/s. Red and blue rectangles mark the heated and cooled fins, respectively. The black dashed lines mark the position where three views (left, central and right) are joined, (b) Normalized local temperature distributions at two positions 1 mm away from the "joint" between the hot and cold fin*

The temperature profiles such as these presented in Figure 20b allow the calculation of the local, phase-dependent heat fluxes on the fin surface. This local, phase-dependent heat fluxes can be integrated over time and space to get the space-cycle averaged heat flux. Figure 21a shows this heat flux q, measured on the first heat exchanger set when the temperature difference is 170°C at different Reynolds numbers.

The same procedure can be applied to obtain the dimensionless heat transfer number (Nu), starting from a local phase-dependent Nusselt number and then integrating this over time and space. Figure 21b shows the space-cycle averaged Nu, measured on the first heat exchanger set, for 170°C temperature difference.

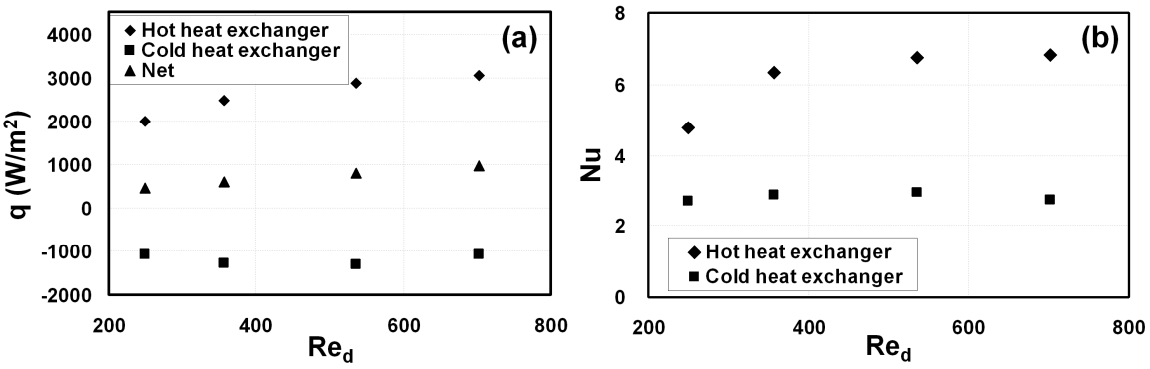

Figure 21 *The dependence of space-cycle averaged heat flux (a) and Nusselt number (b) on Red for the first HX set*

Study of heat exchangers in macro-scale

The idea behind the macro-scale research is to study the influence of the heat exchanger type and dimensions on the heat transfer performance in terms of the heat transfer rate per unit of heat transfer area (the heat transfer coefficient) on the gas side that is exposed to the oscillatory flow. The fin-and-tube type heat exchanger is chosen for this study for its similarity to the configuration of parallel plate/fins in the micro-scale study.

The rig for oscillatory flow measurements is designed as a standing wave arrangement to ensure a large range of displacement amplitudes for the heat transfer studies (Figure 22). The resonator is filled with helium at room temperature and a mean pressure up to 40bar. The operating frequency is 56 Hz, the fundamental resonance frequency of the rig. The heat exchangers are placed next to each other. In each of the three cross sections (both sides of the heat exchanger pair, and in between the two heat exchangers, Figure 22), three thermocouples (evenly distributed in the radial direction) are installed to measure the gas temperature. Thermocouples are also installed to measure the water temperature at inlet and outlet of both heat exchangers installed. The volume flow rates of water through both heat exchangers are also measured.

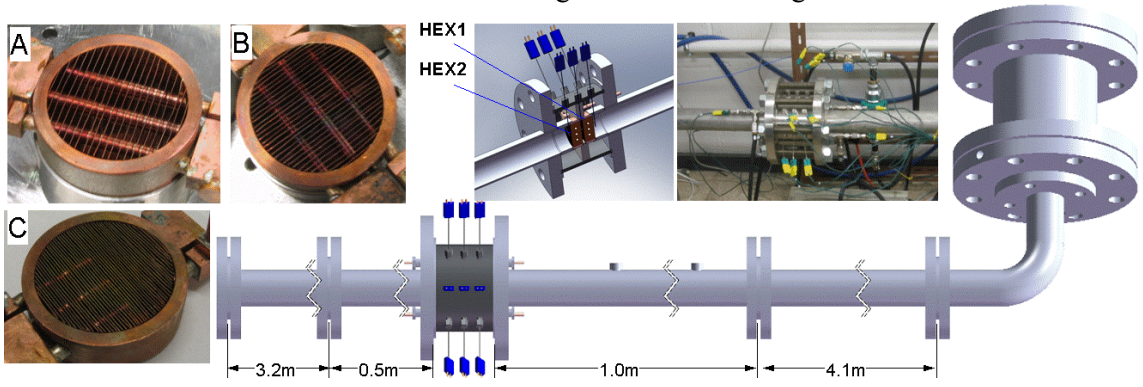

Figure 22 *Heat exchangers A, B, C (left); drawing of the high pressure helium rig and a cut-away view of the test section (right)*

Three fin-and-tube heat exchangers have been designed and constructed with three different fin spacings (0.7, 1.4, and 2.1 mm). The idea behind choosing only three geometrical configurations is that many more experimental cases can be obtained by tuning the mean pressure to obtain different ratios of fin spacing to thermal penetration depth. During the measurement, two out of three heat exchangers are placed in the test section. One heat exchanger is heated by the hot water flow while the other is cooled by the cold water flow. The temperatures of the hot and cold water baths are maintained at around 80°C and 30°C, respectively. The temperature difference between the hot and cold heat exchangers and the ambient is kept low to reduce the heat leakage that may distort the heat transfer measurements.

The measured heat transfer coefficients, represented by the Nusselt number are plotted against the acoustic Reynolds number for all three tested heat exchangers. Some of the macro-scale tests have been repeated in the improved condition and data are being further analysed. Figure 23 shows some sample data obtained in the macro-scale experiments.

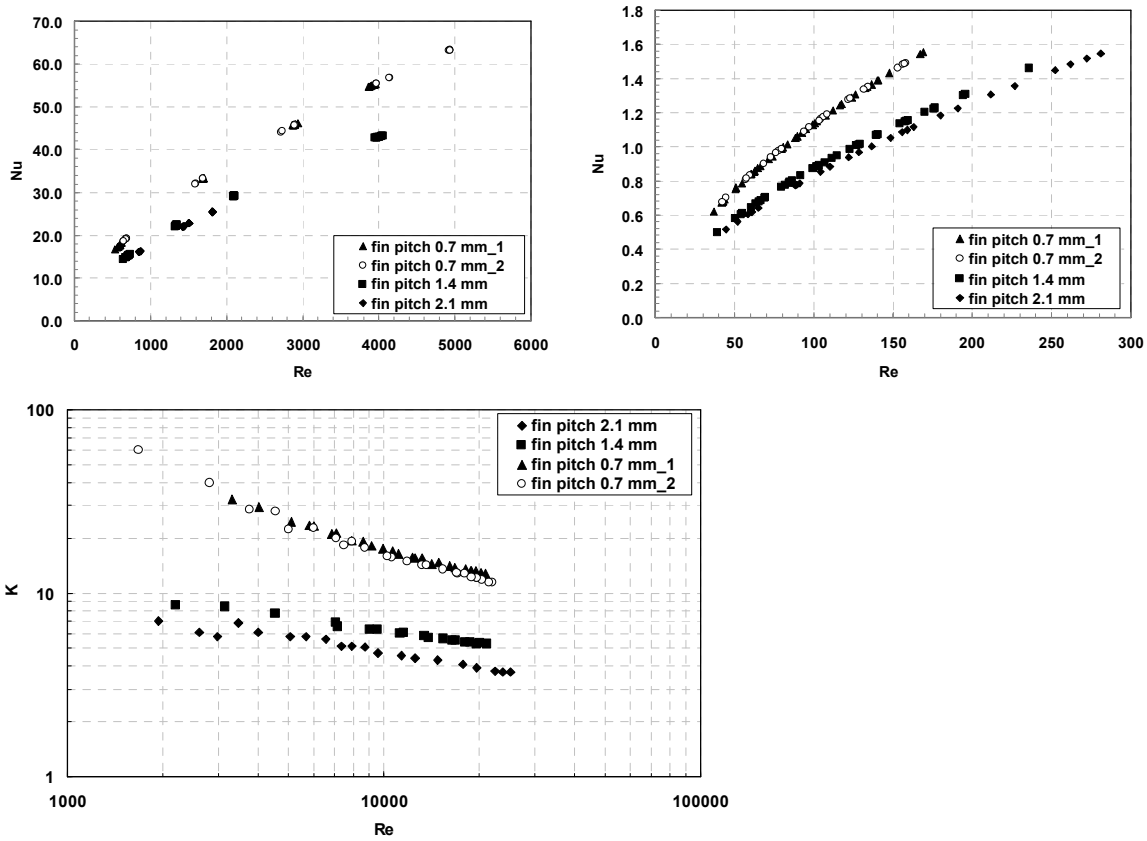

Figure 23 *(a) Heat transfer performance on the air side in steady flow test; (b) Heat transfer performance on the water side in steady flow test; (c) Flow resistance on the air side in steady flow test. Data to be further used in the analysis of the data from the oscillatory flow tests*

3.5.2 CFD modelling

This task addresses the need to develop a numerical scheme for the predictions of the heat exchanger performance in oscillatory flow conditions and to validate the CFD model based on the experimental results collected. CFD modelling and thermoacoustic modelling is divided into a detailed micro-scale and macro-scale modelling of the heat exchanger. The two modelling approaches enable a study of local and time resolved (micro-scale) as well as global (macro-scale) heat transfer characteristics of heat exchangers and generation of appropriate result databases. The results obtained from detailed CFD simulations, in conjunction with the experimental work carried out, will be used to derive suitable correlations.

Modelling of heat exchangers in micro-scale

The modelling of heat exchangers in micro-scale focuses on a single "periodic segment" (fin and surrounding flow channel in the heat exchanger) by solving the Navier-Stokes equation and energy equation, to simulate the transient fluid flow and heat transfer between the gas and the solid (fins) with high temporal resolution. The velocity and temperature data obtained is further used to derive quantities such as the heat flux and Nusselt number. Commercial software ANSYS Fluent-6.3 is used for simulation.

A sample result is presented for six chosen phases in Figure 24. The temperature and velocity fields from experiments (upper plots) are compared to the simulation results (lower plots).

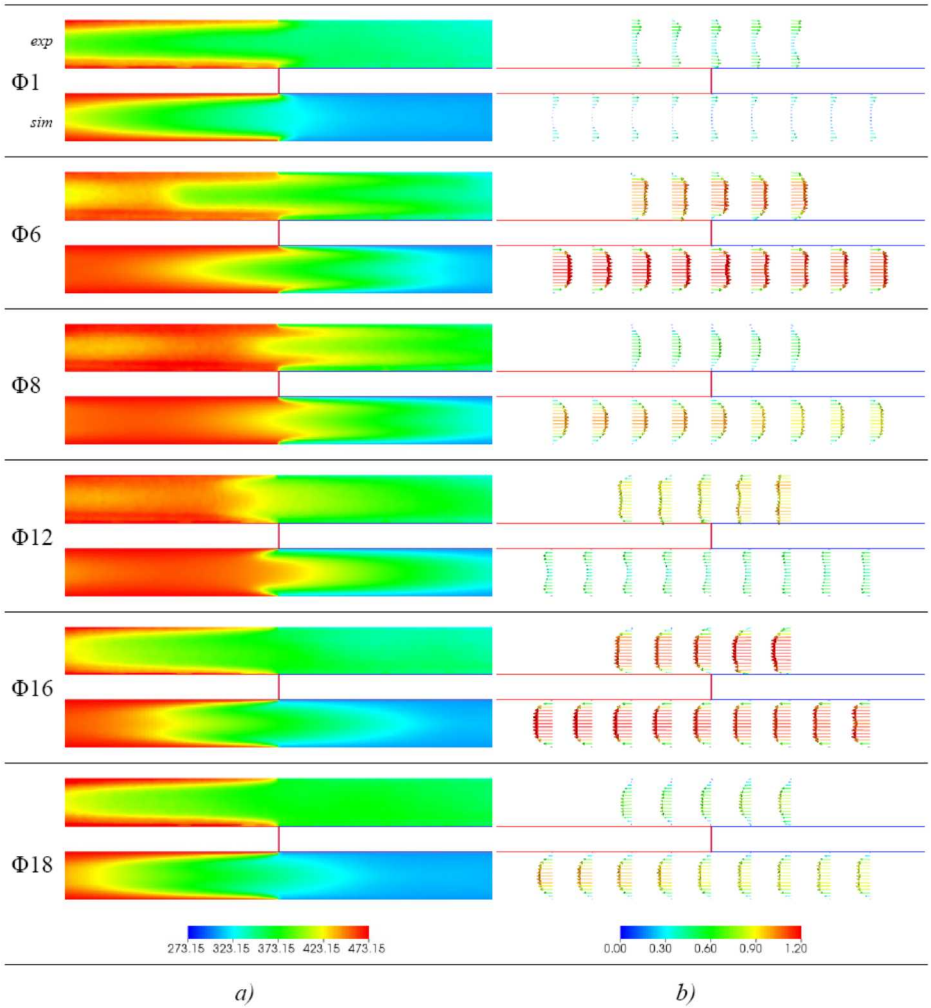

Figure 24 *Temperature (a) and velocity (b) fields from experiment (upper plots) and simulation (lower plots) at Reynolds number of 250 (velocity amplitude 1.30 m/s)*

The heat flux at the wall is calculated for every phase and every location. Then, the local phase-dependent heat flux is used to further calculate the local phase-dependent heat transfer coefficient and the local phase-dependent Nusselt number. The phase-dependent temperature at the centre of the channel at the "joint" section is taken as T_{ref}. A space-cycle averaged Nusselt number is obtained by averaging the local phase-dependent Nusselt number over time and space.

Several important findings can be summarized as follows: (i) A good agreement of the velocity field was found between the simulation and experiments at both acoustic oscillation amplitudes; (ii) The temperature fields from both the simulation and experiments match in trend, but there is a mismatch in values. This is considered mainly due to the heat accumulation in the experimental setup.

Modelling of heat exchangers in macro-scale

This deals with macro-scale modelling of the heat exchanger thermal performance. It employs an energy-balance model, instead of solving the Navier-Stokes and energy equations used in the "micro-scale" approach. Integration of momentum, continuity and energy equations in each sub-system segment is executed through standard numerical techniques with pressures and volumetric velocities matched at the junctions between segments. The model enables estimation of the dependence of the heat transfer rates on quantities such as heat exchanger fin length and

fin spacing in relation to the operating acoustic frequency, drive ratio and mean pressure. The code developed provides an interface for CFD studies of the whole thermoacoustic systems, in particular components such as the regenerator and resonator.

Figure 25 illustrates an example of the time-averaged temperature field in the computation domain when the Reynolds number is 304, and the corresponding transverse heat flux density. The heat flux exhibits a sharp peak near the fin ends indicating that a net heat exchange between fluid and solid takes place in these regions. In particular, the maximum value is reached when the fin edges are approached. From the calculated time averaged temperature distribution, the heat loads on the cold and hot heat exchangers as well as the time averaged Nusselt numbers have been deduced for Reynolds number (Re) ranging from 100 to 800, see Figure 26. The effects of important design parameters, such as fin length along the particle acoustic oscillation and the fin spacing (Figure 27), on the heat transfer performance of the heat exchangers are then investigated. Figure 28 shows the mean heat flux per surface area along the length of the heat exchanger-stack assembly.

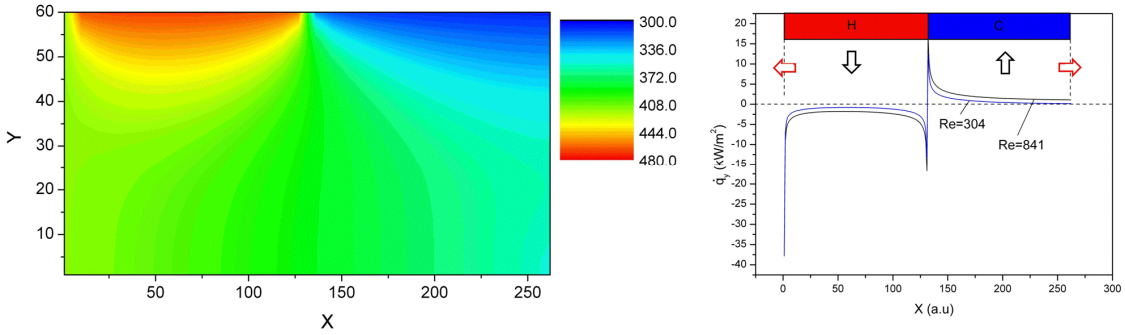

Figure 25 *Time-averaged temperature distribution (left) and transverse heat flux density (right). Re=304*

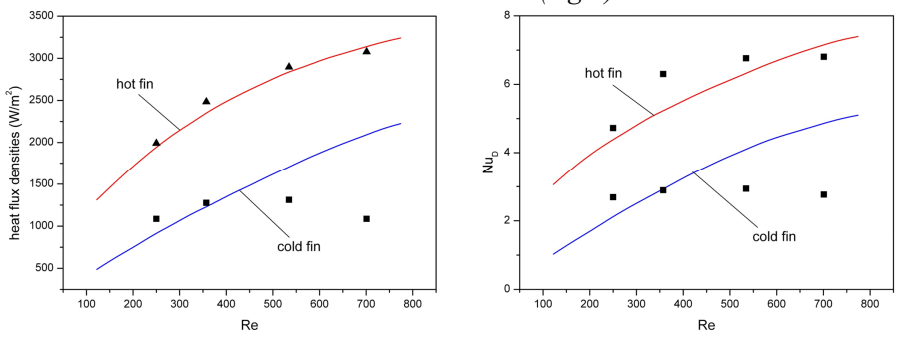

Figure 26 *Dependence of space-cycle averaged heat flux, Nusselt number on Re for the 1st set of heat exchangers*

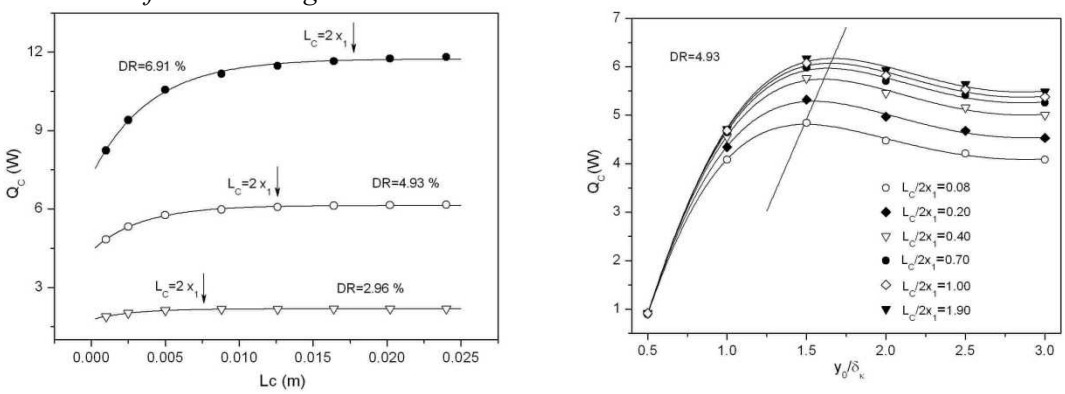

Figure 27 *The cooling load as a function of the length (left) and fin spacing (right) of heat exchangers*

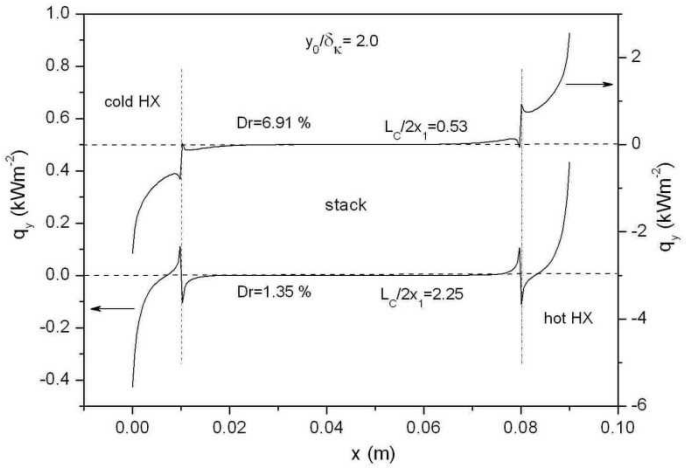

Figure 28 *The mean heat flux per unit surface area exchanged by the cold fin with the gas at selected drive ratios*

The following conclusions were drawn:

- The magnitude of the heat transfer coefficient from the secondary fluid-side (U) should be fully taken into account because it affects cooling load through its influence on the temperature distribution across the stack. High U values are desirable to improve the performance of the device.
- Fin length along the axial direction of particle oscillation can be chosen considerably lower than the peak-to-peak displacement amplitude without compromising the heat exchanger performance and with great benefits in terms of viscous losses reduction.
- Thermal losses (reverse heat fluxes) localized at the stack-heat exchanger junctions degrade the HXs performance reducing the useful cooling load. These effects could account for about 7% of the deviations found between predictions of the linear theory and experimental measurements. Suitable choices of the fin spacing and fin length can contribute to minimize this detriment effects enhancing the effectiveness of the heat exchangers.
- Optimum fin/plate interspacing should fall in the range $2\delta_\kappa \leq 2y_0 \leq 4\delta_\kappa$. Selection of the best value is case dependent and should also take into account the simultaneous effect of blockage ratio, fin length and fin thickness.
- Heat transfer coefficients from the gas-side can be predicted with a confidence of about 41% at moderate acoustic Reynolds numbers.

Non-dimensional correlations of heat transfer processes in oscillatory flows

The non-dimensional analysis of heat transfer from the parallel-plate heat exchanger to the oscillatory flow has been carried out. Nusselt number as a function of a group of non-dimensional parameters has been studied. Sample data are presented in Figure 29.

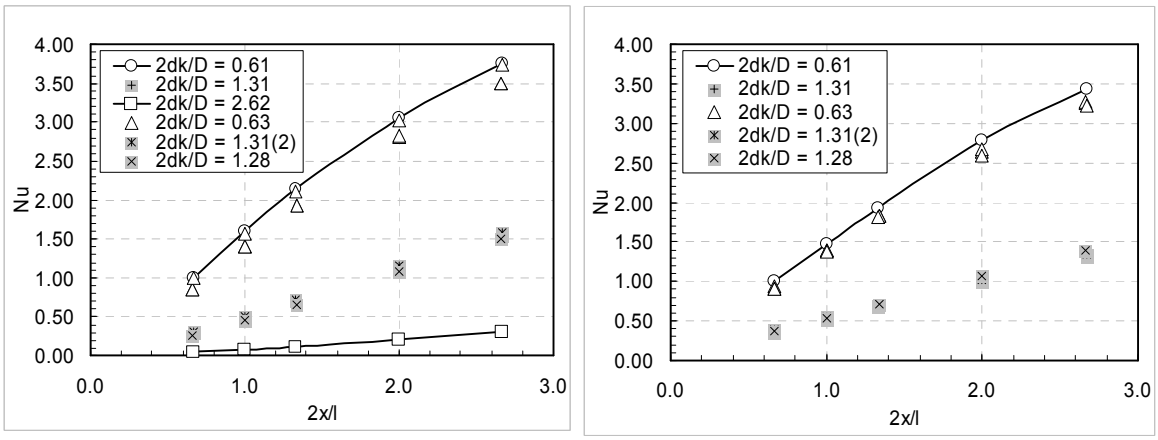

(a) (b)

Figure 29 *(a) The dependence of Nusselt number on 2δκ/D, l/ξa (macro-scale CFD model); (b) The dependence of Nusselt number on 2δκ/D, l/ξa (micro-scale CFD model)*

The results from macro- and micro- scale CFD models are in good agreement. Both suggest that the heat transfer performance is better when $2\delta_\kappa/D$ has a value around 0.6, within the range used in the study. Nevertheless, the result also suggests that the Nusselt number almost linearly increases with $2\xi_a/l$. In comparison, the cooling load will not further increase with $2\xi_a/l$ when $2\xi_a/l$ is more than 1.

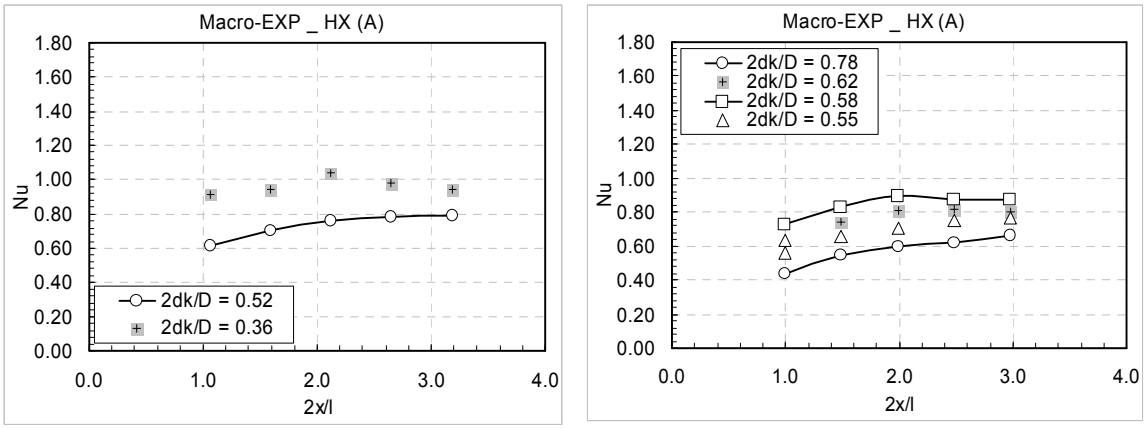

Figure 30 *The dependence of Nusselt number on 2δκ/D, l/ξa (old macro-scale experiment)*

The experiment suggests that the heat transfer performance is better when $2\delta_\kappa/D$ has a value around 0.36, lower than what is suggested by simulation. Furthermore the Nusselt number does not increase further with $2\xi_a/l$, when it is over 2.0. The conflict between the experiment and simulation needs further investigation.

3.5.3 Design of practical heat exchangers

This task focuses on two aspects of the overall project. Firstly, it will be necessary to propose the optimal parameters for the heat exchangers used. Secondly, given the ultimate aim of the project which relates to the application of the "emerging technology" in a wider market context, it is necessary to make a detailed analysis of the available fabrication techniques for thermoacoustic heat exchangers, and to develop costing guidelines for various heat exchanger implementations, and to provide detailed recommendations for future technological approaches to heat exchanger manufacturing..

Several practical heat exchangers have been built in the framework of the THATEA project, each kind of device was made in a very low number of units. The efficiency criterion led to use validated technologies without optimizing the device cost (except in the case of low temperature

engine). Hence, the unit production and the use of special technologies induced very large costs for the heat exchangers building. For an intermediate production volume (1000 units), the manufacturing cost may be reduced by an important factor, but it is not possible to extrapolate the cost for a mass production: in the latter case, cheaper mass production methods would be used and one could thus expect costs reduction. Many ways of machining could be explored as:

- the Electric Discharge Machining (EDM) work is the most difficult part of the production but it could be automated. However, other cheaper means to make the heat exchanger can be thought of like chemical etching;
- the tooling has an important impact on a unit fabrication cost but it will be negligible for mass production.

To define some recommendations concerning the technological approaches and the industrialization of the heat exchangers used for the thermoacoustic applications, the heat exchangers build for the THATEA project were evaluated by means of the following criteria: fabrication price, thermal transfer efficiency, pressure drop. The criteria values obtained with THATEA heat exchangers are given in Table 4.

Table 4 *Characteristics of THATEA heat exchangers*

Technology kind	Heat transfer coefficient (fluid side)	Heat transfer coefficient (thermoacoustic side)	Pressure drop (fluid side)	Price
Tube-Fin	28 W/K	40 W/K	1 300 Pa	210 €
Tube-Shell	80 W/K	210 W/K	40 000 Pa	4 900 €
Fin-Fin	43 W/K	100 W/K	1 400 Pa	5 000 €
Tube-Fin	100 W/K	250 W/K	5 000 Pa	5 300 €
Tube-Shell	130 W/K	280 W/K	25 000 Pa	5 500 €
Fin-Fin *	14 W/K	275 W/K	2 000 Pa	15 000 €

* This heat exchanger operates at high temperature T > 600 °C.

One partner has used an industrial technology (similar to car air condensers) leading to a poor heat transfer efficiency in a thermoacoustic configuration but yielding the lowest construction cost of the project. The technologies applied for the other heat exchangers involve a cost on average twenty times higher. These prices are not representative of an industrial production because only one or two heat exchangers of each kind have been built. For the THATEA project, the thermal performance criterion is privileged; this choice involves the development of new devices and raises the fabrication price.

The adaptation of an existent industrial device seems a good way to reduce the manufacturing cost and allow for a mass production, but the geometrical constraints reduce the kinds of technology usable in the thermoacoustic applications. For example, the thermal transfer performances of tube-fin heat exchangers used in the low temperature engine are not enough to obtain a good energetic efficiency of those thermoacoustic machines.

Compact heat exchangers are widely used in the refrigeration industry where they are produced massively and their performances thus well known. These configurations have a very high surface area density per unit volume with small hydraulic diameter and these characteristics seem to fit well the acoustics constraints. The supplementary motivation for using compact heat exchanger is to gain specified heat exchanger performance, within admissibility mass and volume constraints.

In several recovery energy applications and particularly for the embarked applications, the mass of the machine is an important parameter and the use of material having weak densities (like Aluminum…) should be privileged. Moreover, the efficiency of machines is improved when the mass is reduced.

For the high temperature applications, the environment constraints are severe. The technology and the material used (refractory steel, Ni alloys) are expensive. The reduction of cost production will be more limited in comparison with the ambient temperature applications.

3.6 Resonators

In a thermoacoustic system the function of the resonator is to determine the operating frequency, to store the acoustic energy to be amplified by the thermoacoustic engine and to transfer the output power of this engine to the acoustic load which could be either a heat pump or cooler as well as an alternator. Acoustic losses in the resonator can seriously affect system performance in particular at medium and low operating temperatures. Two different options were pursued with the aim to reduce the resonator losses compared to the useful acoustic power.

3.6.1 Traveling wave resonator

An analysis is performed of acoustic loss in all possible implementations of acoustic resonance and feedback circuits like ½ λ and ¼ λ standing wave, traveling wave and hybrid configurations. Calculated values are compared with experimental data from literature. For some new configuration for which no data was available experiments are performed to validate the calculation results.

Coupling efficiency is defined as the ratio between power available at the load and the (equivalent) source power. This coupling efficiency is calculated and ranked for all configurations emanating from operating conditions for engine and heat pump or cooler as agreed in work package 6.

In this analysis it is found that, for the same operating conditions of engine and heat pump, acoustic losses in a mechanical resonator and in a traveling wave feedback loop are significant lower as compared with the commonly used standing wave type resonator with a torus or bypass type engine or heat pump. The mechanical resonator is studied in task 4.2. The traveling wave feedback loop is further investigated within this task. A small scale experiment at atmospheric pressure with a 4-stage thermoacoustic engine utilizing the traveling wave feedback circuitry is given in Figure 31.

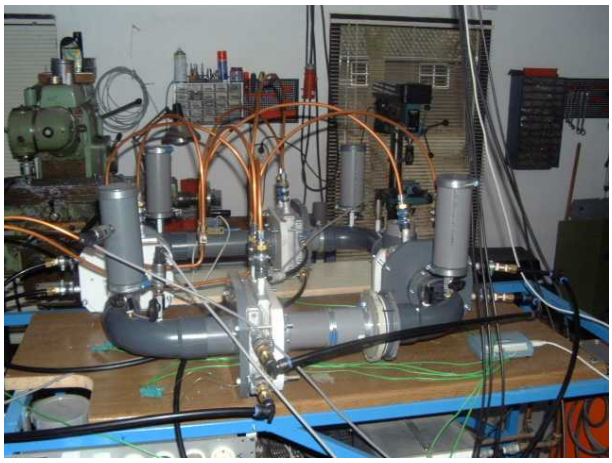

Figure 31 *Small scale experiment of travelling wave feedback in a four stage thermoacoustic engine*

The experiment validated the traveling wave approach by showing indeed a very low onset temperature and a steep increase of acoustic loop power with temperature difference applied. In addition to the low loss the internal gas volume is found to be more than a factor of five less than the internal volume of the standing wave version for the same operating conditions yielding a more compact system. This is particularly important for low temperature systems. In addition, the combined loss analysis of continuous and oscillatory flow performed in this task

has yield a better understanding of the impact of wall roughness. This roughness is of minor importance for the losses of the configuration presented here.

3.6.2 Mechanical resonator.

A mechanical resonator is one of the options to reduce resonator losses and to realise more compact systems. The mechanical resonator was studied in two ways. An inventory was made of possible concepts and experimental work was carried out on a mass-spring system.

Inventory

In addition to the experimental work an inventory was made of acousto-mechanic resonators configurations. There are roughly two different approaches : the first one is using bellows as oscillating device, the second one uses springs as oscillating device. Three designs for acousto-mechanic resonators are shown below in Figure 32.

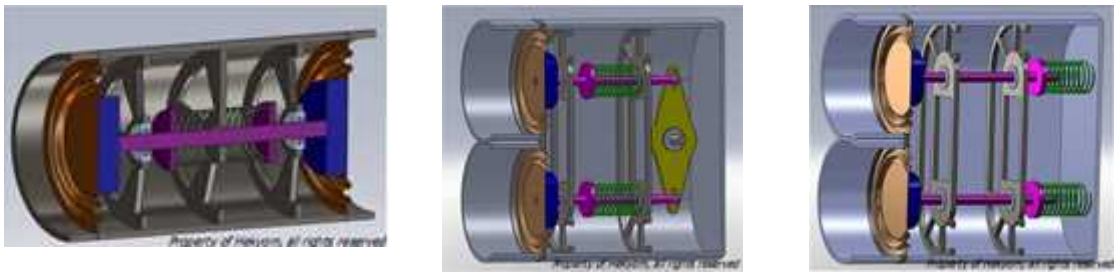

Figure 32 *Spring axial resonator (left) ; spring non-axial resonator with a connecting rod transmission (middle), spring non-axial resonator with a fluid transmission (right)*

In the three cases, the oscillating device is realized with a spring linked with a piston or membrane. The mechanical resonance frequency and the mechanical impedance at the two membranes must match respectively the acoustical frequency and the acoustical engine impedance. In the left design, the piston motions are in phase, leading to external vibrations. In order to avoid these vibrations, the motions of the two devices presented in the middle and right design are opposite in phase. The motion transmission is realized on the left by a connecting rod and on the right by an incompressible fluid. For the right design, some calculations were carried out to estimate the viscous losses in the fluid. These losses seem to be minor.

Experiments

In the scope of this task a compact mechanical resonator (mass-spring) is designed and build. This mechanical resonator should be tested using an existing thermoacoustic Stirling engine. A twin mass-spring system is chosen to minimize vibrations. An illustration of the mechanical resonator attached to the thermoacoustic engine is shown in Figure 33.

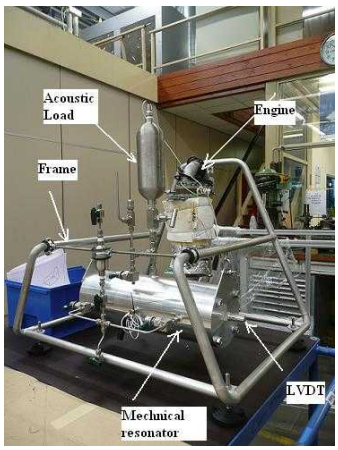

Figure 33 *Picture of the mechanical resonator attached to the thermoacoustic engine*

Unfortunately, the mechanical resonator did not start when coupled to the thermoacoustic engine. The system has too much damping. Possible causes were identified as (1) damping in the spring plates, (2) losses the seal gap, (3) rubbing of the displacement sensors, or (4) a slight unbalance between both resonator halves.

The damping in the spring plates was checked independently by use of a mechanical shaker. These measurements show a very low damping of the springs. The diameter of the displacements sensors was reduced to prevent rubbing. Next, the damping by the seal gap is tested by illustrated in Figure 34.

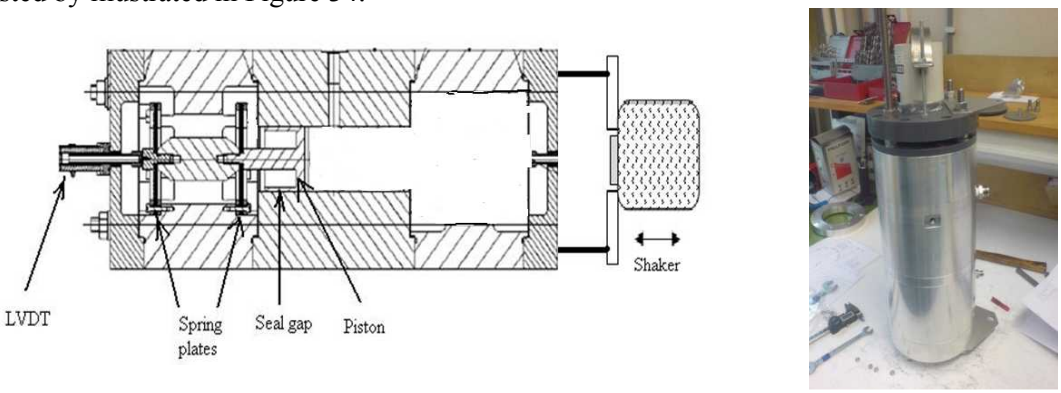

Figure 34 *Set up used to determine the damping of the seal gap. The twin mass-spring systems will be tested separately*

Figure 35 shows the resonance peak of the mass-spring system. The points are measurements data and the solid line is a fit to the data. The fit gives a value for the mechanical resistance of 2.55 N.s/m, which is a very low value.

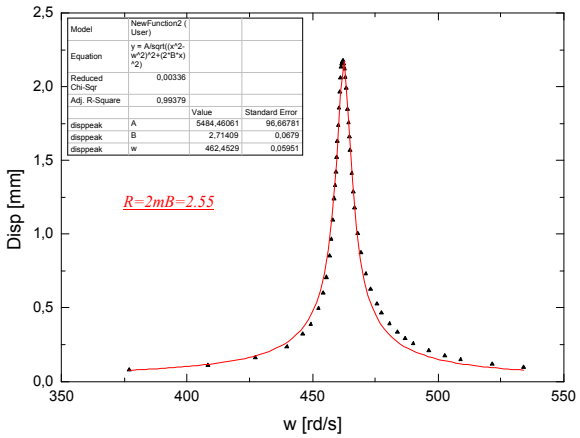

Figure 35 *Displacement of the piston as function of the angular frequency of the driving shaker (resonance peak). The points are measurements data and the solid is a fit expression*

Finally, an alignment of both piston-cylinders is achieved simultaneously. A loudspeaker is used to drive the mechanical resonator. The loudspeaker is connected to the mechanical resonator via the port made for the connection of the TA-engine. Figure 36 shows a picture of the system.

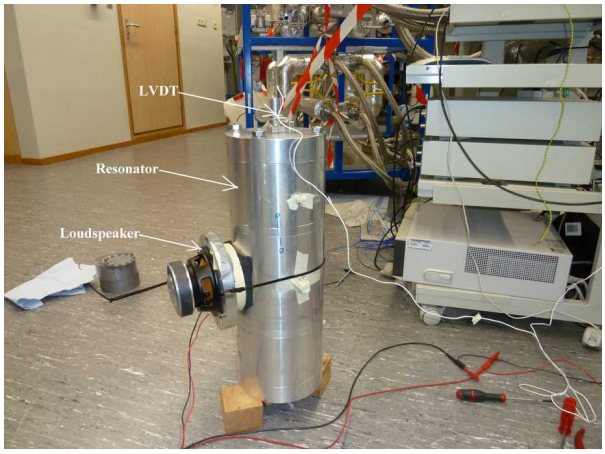

Figure 36 *Picture of the mechanical resonator driven by a loudspeaker.*

The damping for each mass-spring part of the twin mass-spring forming the mechanical resonator is determined by measuring the displacement of the pistons as discussed in the previous sections. The difference with the experiments done so far is that now the two mass-spring systems are coupled. The experiments are done at atmospheric pressure. Figure 37 shows the resonance peak of the mass-spring M1 coupled to mass-spring M2. The deduced mechanical resistance is 2.93 N/m.s which is a little bit higher than the resistance measured when M1 was not coupled to M2. This is believed to be due to the alignment of the piston in the cylinder.

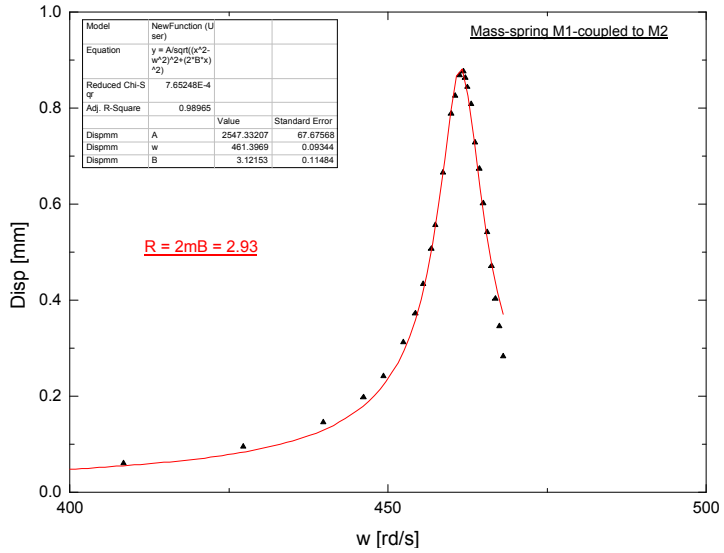

Figure 37 *Displacement of the mass-spring M1 coupled to mass-spring M2 as function of the angular frequency of the driving loudspeaker (resonance peak). The points are measurements data and the solid line is a fit expression (11) to the data the data which gives the mechanical resistance of the system.*

Conclusions

- A study has been performed on different mechanical resonator concepts that look very promising.
- A mechanical resonator is designed and built but could not be tested coupled with a thermoacoustic engine. Separate tests concluded that the misalignment of the pistons in the cylinders is the most probable cause for this. The mechanical parameters deduced from the experiments do not differ much from those used in the design of the system. The alignment of the cylinder in the piston is a very critical issue considering the small clearance seal of 15 μm. An exploration of other ways for alignment is recommended for the further study of the feasibility of a mechanical resonator to replace an acoustic one.

3.7 Non-linear phenomena

The objective of this work package is to develop the fundamental understanding of the non-linear effects of streaming flows in thermal buffer tubes, through carefully designed experimentation; and accompany this with CFD modelling capabilities to capture the physics of streaming flows when the thermal effects are very important and to validate the models against the experimental data.

3.7.1 Experimental research

The experimental setup is built from an acoustic source and a resonator + PIV cell, see Figure 38.

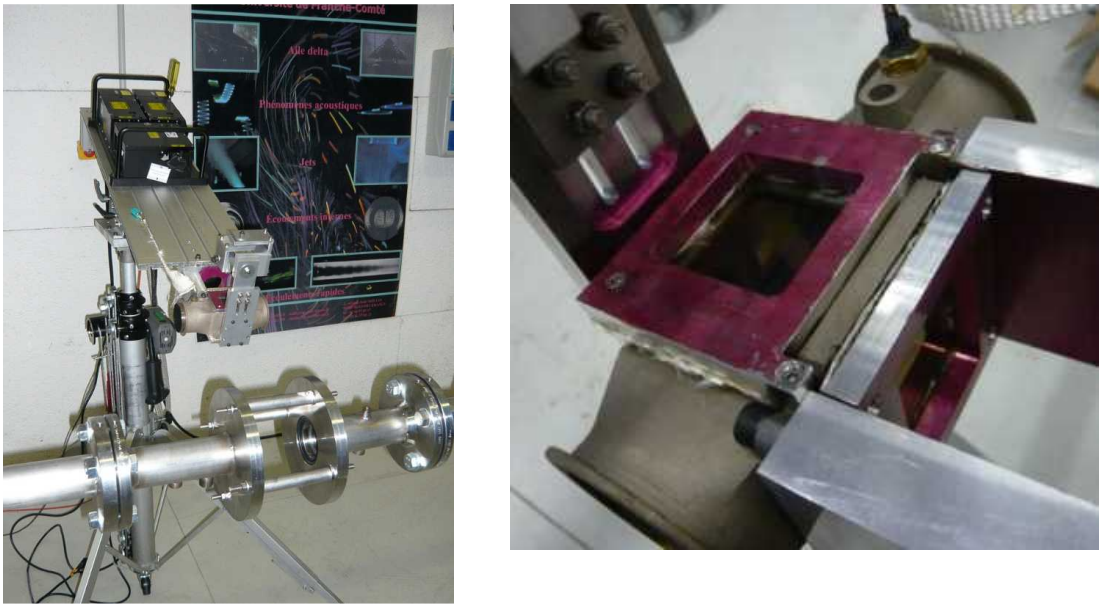

Figure 38 *PIV visualization cell, camera and laser mounted on a tripod. Right: zoom on the visualization cell*

Several transducers were distributed at different locations along the resonator in order to provide pressure field data for the numerical simulations. All the signals are recorded and processed with a sampling rate of 16 kHz. The velocity measurement is achieved thanks to the PIV method. This technique relies on a laser sheet light illuminating particles injected into the resonator. Knowing there displacements from a recorded picture to another, the spatial velocity field in the resonator is therefore known. The piston displacement and the operating frequency of the driver (shaker) can be adjusted. Drive ratio values between 3% and 6% were achieved at a resonance frequency of 25 Hz under atmospheric air pressure.

Table 5 summarises the experiments conditions performed with the shaker. The varying parameter is the piston stroke which modifies the pressure amplitude and thus the drive ratio.

Table 5 *Experimentations conditions*

	Test T1	*Test 2*	*Test 3*	*Test 4*
P_1 (mbar)	34	42	49	56
P_1/P_m (%)	3,3	4,2	4,8	5,5
Piston stroke (mm)	7,07	8,48	9,90	11,3

With P_1: acoustic pressure

The following figure (Figure 39) presents the streaming velocity profiles for different drive ratios. Two conclusions can be drawn: the acoustic streaming amplitude increases with the drive ratio and one Rayleigh cell is present.

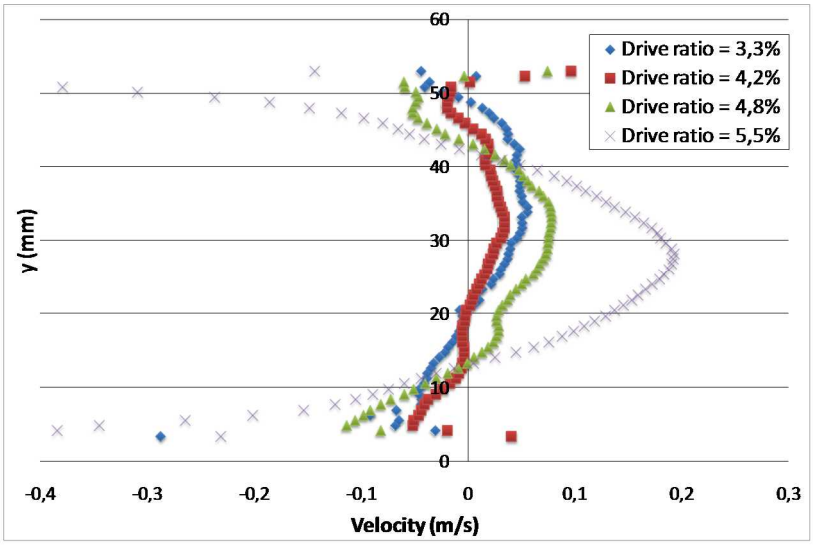

Figure 39 *Streaming velocity for different drive ratios*

Experiments with thermal gradient were carried out adding two heat exchangers (based on tube-and-shell technology) on either side of the PIV module. The heat exchangers were designed at FEMTO-ST. Figure 40 presents the streaming velocity profiles for three different drive ratios and a temperature gradient of 86°C/m. The phenomenon of natural convection appears to prevail on the streaming effect.

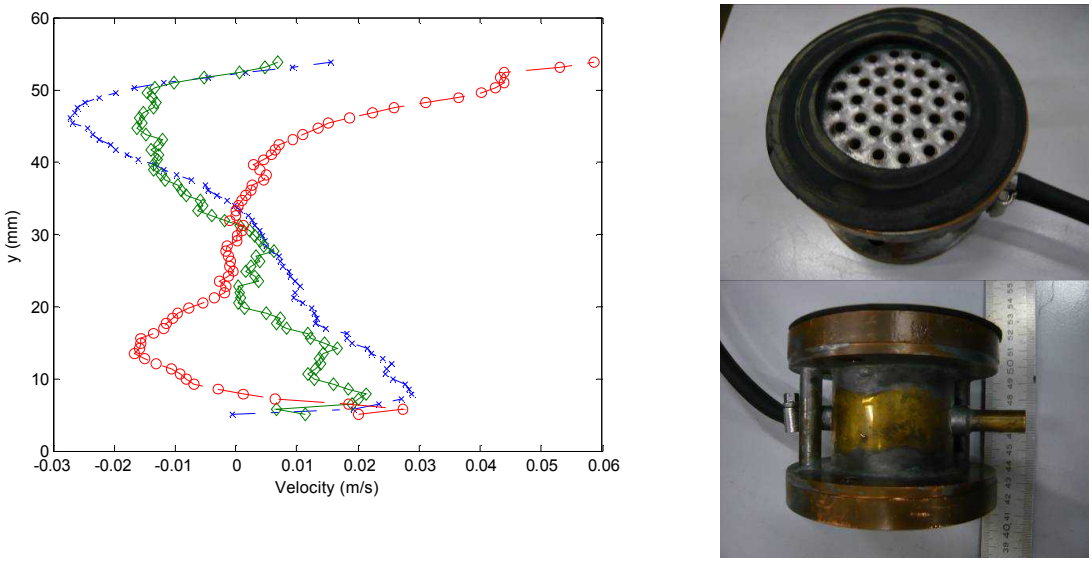

Figure 40 *Streaming velocity profiles with air and for different drive ratios, ×: 1,4%, ◊: 1,8%, o: 3,3%. The heat exchangers are shown to the left*

Conclusions

One of the first objectives of this work package was to design an experiment capable of measuring acoustic streaming inside the resonator.. The experimental apparatus proved to be efficient and consequently the measurement method was validated against numerical study. The experimental set-up was later equipped with two heat exchangers, in order to set the temperature gradient and to reach the conditions found in thermoacoustic systems. This situation requires further study as the desired conditions cannot be reached in the present setup.

3.7.2 CFD model research

The experimental results were used to validate CFD for modeling of streaming phenomena. The comparison showed a good qualitative agreement but less agreement quantitatively. Since the

trends were predicted correctly, CFD was applied to a real system to address the streaming phenomena that occur in those systems. This would provide insight in the time-averaged processes that take place.

A realistic geometry of an engine consisting of a toroidal tube and a resonator is considered. The torus contains the actual engine part, it consist of are the cold and the hot heat exchangers, and regenerator included between them. The ambient heat exchanger is situated below engine part in the thermal buffer zone, which connects toroidal engine parts via a T-junction with the rest of the system. In every fluid flow oscillation, the flow passes through these regions and it is heated via the gradient of temperature imposed in the regenerator.

Figure 41 *Toroidal engine with resonator*

Helium gas at operational pressure of P_m = 40 bars is used in the setup. The temperatures of heat exchangers were set to 300 and 600 K respectively.

In the experimental devices a flexible membrane is installed in the torus to prevent Gedeon-type streaming (also called “dc flow”). It is quite challenging to simulate such a membrane with CFD, therefore we choose another approach to suppress the dc flow. The resistance in the regenerator region was altered depending on the flow direction, i.e. the downward flow experienced higher resistance than upward. The ratio between the two was adjusted manually to reach zero streaming velocity in the engine

Here, we concentrate on the secondary flow within the thermal buffer tube. In the absence of Gedeon-type streaming, the flow is driven by boundary-layer effects and usually referred as Rayleigh streaming. Two vertical and two horizontal planes were chosen for analysis. The results are shown in Figure 42. The figure shows a clear circulating flow pattern within the thermal buffer tube. This pattern seems to be driven by the flow splitting a the T-branch. The circulation does not reach the upper heat exchanger, so the convective heat loss from this heat exchanger due to the circulation is limited.

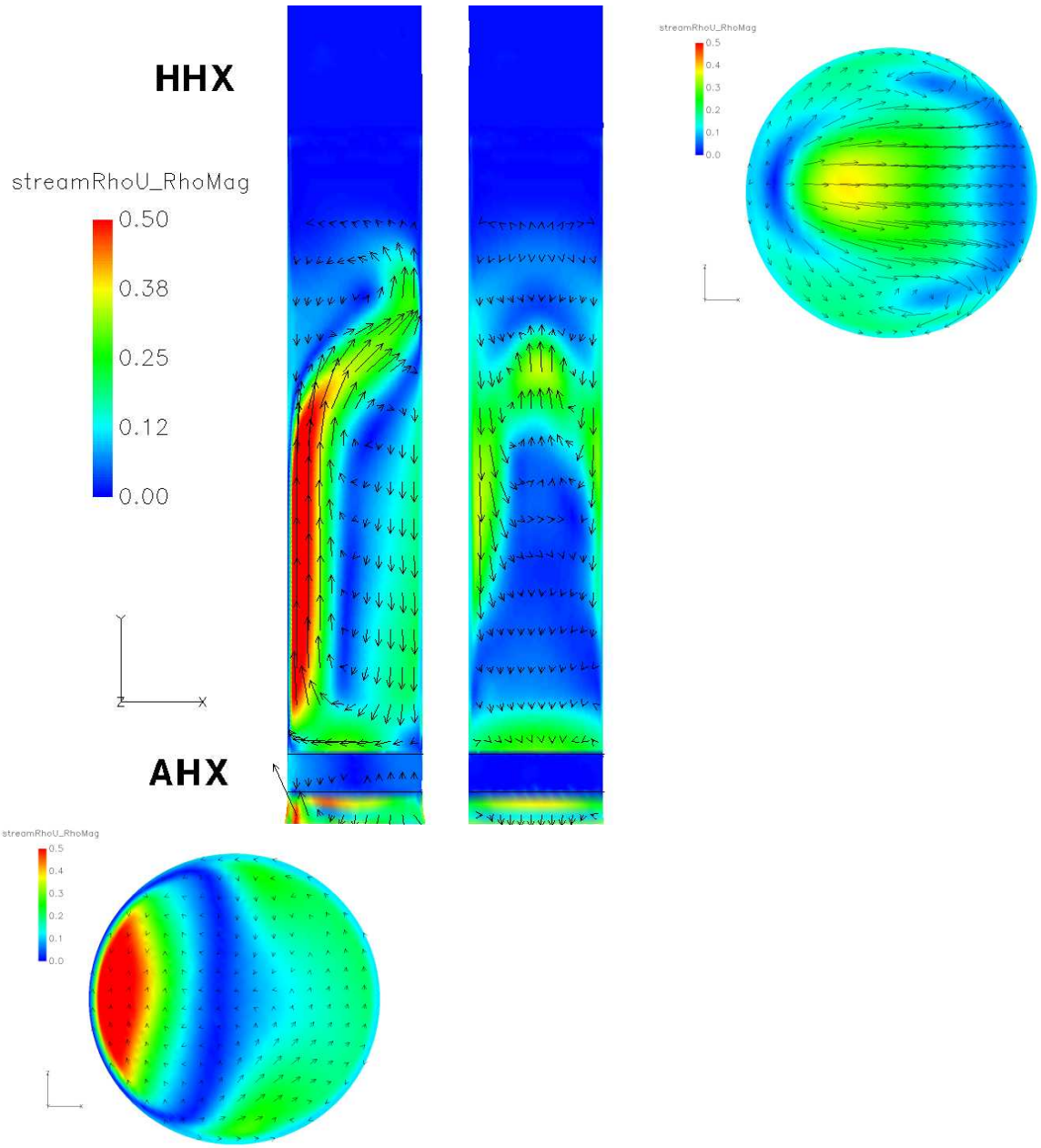

Figure 42 *Streaming patterns in the thermal buffer*

Conclusions
The data has been used to validate CFD modeling. The qualitative agreement was reasonable but the quantitative agreement should be improved. CFD modeling proved to be a useful tool to study the time-independent phenomena that occur in oscillatory flow conditions. A thorough understanding of these phenomena is needed to identify countermeasures that stop streaming. This subject definitely requires further research.

3.7.3 Streaming reduction measures

A theoretical study was carried out to identify measures to suppress streaming. The phenomena of streaming are many, depending on the geometry of the system, the operating conditions and the thermal levels. To talk about ways to reduce the flow amounts to make a case-by-case study requiring different but always complex experimental bench for validation. Thanks to studies on

experimental facilities and numerical analysis of phenomena, it is known that the methods used at present for the reduction of "streaming" are:

- Use of a working fluid with low Prandtl number
- Balance the pressure gradient created by the use of conical tubes (Rayleigh streaming)
- Insert elements to rectify the flow
- Introduction of a flexible membrane in the acoustic circuit (streaming of Gedeon)
- Introduction of devices that generate a pressure gradient opposite to the streaming ("jet pump" (streaming of Gedeon)
- Active control of acoustic flow

3.8 Integral systems

Objective of this work package is to demonstrate two integral systems, composed of a TA engine coupled to a TA heat pump. These two different integral systems will represent two different (industrial) applications.

3.8.1 High-temperature integral system

This activity concerns the coupling of the high temperature thermoacoustic engine to a high temperature thermoacoustic heat pump operating between 10°C and 60°C or 80°C. The heat pump is designed, built, attached to the engine, and the integral system is tested. A CAD-drawing and a picture of the heat pump are shown in Figure 43 and a picture of the integral system is shown in Figure 44.

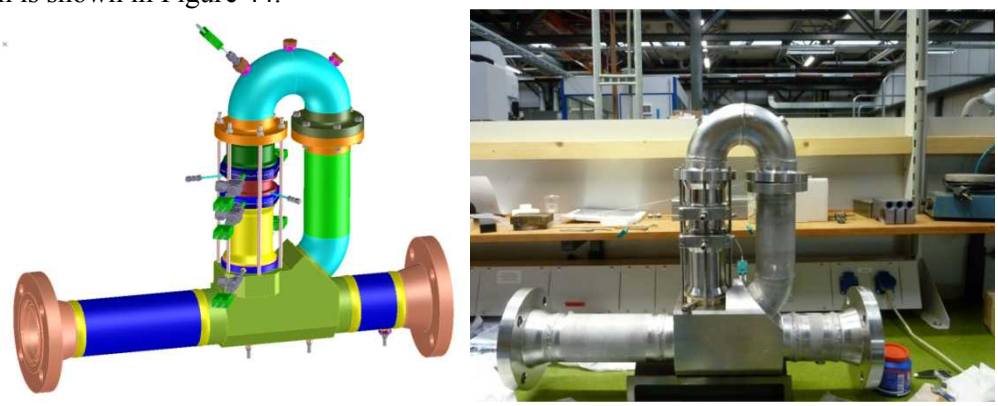

Figure 43 *CAD-illustration (left) and picture of the heat pump (right)*

Figure 44 *Picture of the high-temperature thermoacoustic integral system*

The overall performance of the integral system is given in Figure 45. The integral system achieves an overall performance of 0.92 for a medium temperature of 60°C and a performance

of 0.81 at 80°C. This is lower than the objective performances for both cases which are 1.4 and 1.2, respectively.

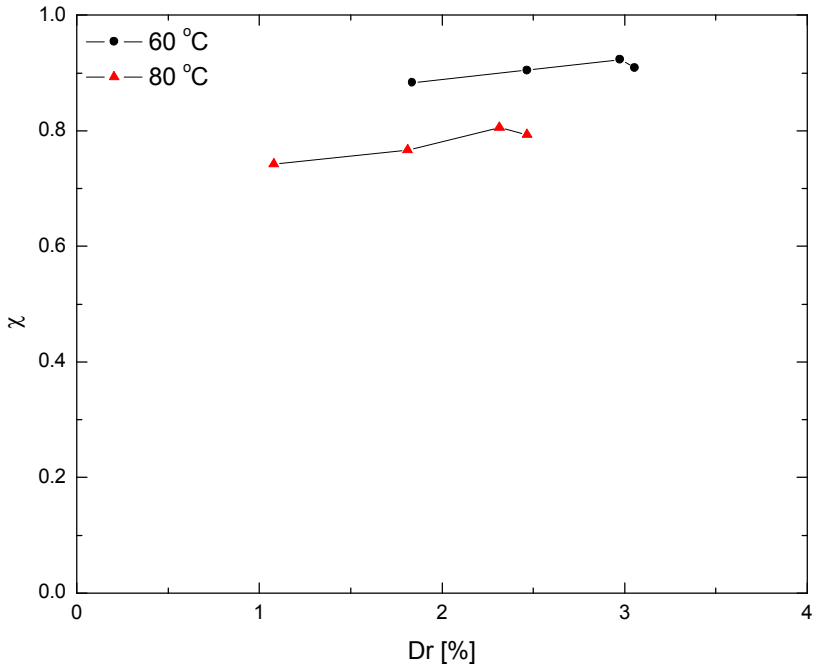

Figure 45 *Overall performance of the high-temperature thermoacoustic integral system for two medium temperatures 60 and 80°C*

The project objectives and the achieved results for the integral system at a drive ratio of 2.47 % are summarized in Table 6 and Table 7 for 60°C and 80°C, respectively.

Table 6 *Objective and achieved results for the high-temperature integral system for 60°C*

	Project plan	Achieved
Efficiency relative to Carnot engine	0.40	0.24
Performance relative to Carnot Heat pump	0.40	0.39
Performance integral system	1.40	0.92
Resonator efficiency	0.90	0.75

Table 7 *Objective and achieved results for the high-temperature integral system for 80°C*

	Project plan	Achieved
Efficiency relative to Carnot engine	0.40	0.21
Performance relative to Carnot Heat pump	0.40	0.39
Performance integral system	1.20	0.81
Resonator efficiency	0.90	0.76

This lower performance is due to the large heat losses in the engine. If we would be able to suppress the heat leak down the TBT for example results in an overall performance of 1.2 at 60°C and 1.1 at 80°C. Additionally, the performance of engine increases with the drive ratio. In the resent experiments it is not possible to achieve higher drive ratio's than about 4 % because of the limited heat input to the engine as a consequence of the heat losses and limited hot air flow. Higher efficiencies can be achieved by suppressing or minimizing the heat leak and improving the heat transfer of the hot heat exchanger in the engine.

In the integral system at dr = 2.47 % the heat pump achieved a performance relative to Carnot of 39 % for both temperature of 60 and 80°C but the engine efficiency is significantly lower. The resonator achieved a performance of 76 % at dr = 2.47 %.

Conclusions

The integral system achieves an overall performance of 0.6 for a medium temperature of 60°C and a performance of 0.5 at 80°C at dr = 2.47 %. This is lower than the objective performances for both cases which are 1.4 and 1.2, respectively. This lower performance is mainly due to the large heat losses in the engine. Additionally, it is shown in this document that the performance of engine increases with the drive ratio. In the present experiments it is not possible to achieve higher drive ratio's because of the limited heat input to the engine as a consequence of the heat losses and limited hot air flow. Higher efficiencies can be achieved by suppressing or minimizing the heat leak and improving the heat transfer of the hot heat exchanger in the engine.

The system reaches about 60 % of the objective. While at the component level the efficiencies are 75 % or higher (even to 100 %) of the target, the multiplication of the efficiencies of the individual components leads to this overall result. The requirements for the optimal performance of the individual components do not always match with each other. For example, a high drive ratio leads to high useful powers compared to the heat losses and thus a high efficiency for an engine but at the same time a high drive ratio leads to high acoustic losses in the resonator

3.8.2 Low-temperature integral system

The refrigerator and low-temperature engine are designed and constructed by different partners in the project and build and tested in different acoustic geometries. To end up with a complete system an integrating strategy was agreed. This integration involves replacing one of the four engine stages of the low temperature engine by the regenerator unit of the refrigerator. This integration strategy is depicted schematically in Figure 46. This approach has been proven to be successful resulting in a full functional low temperature integrated system according to the project plan.

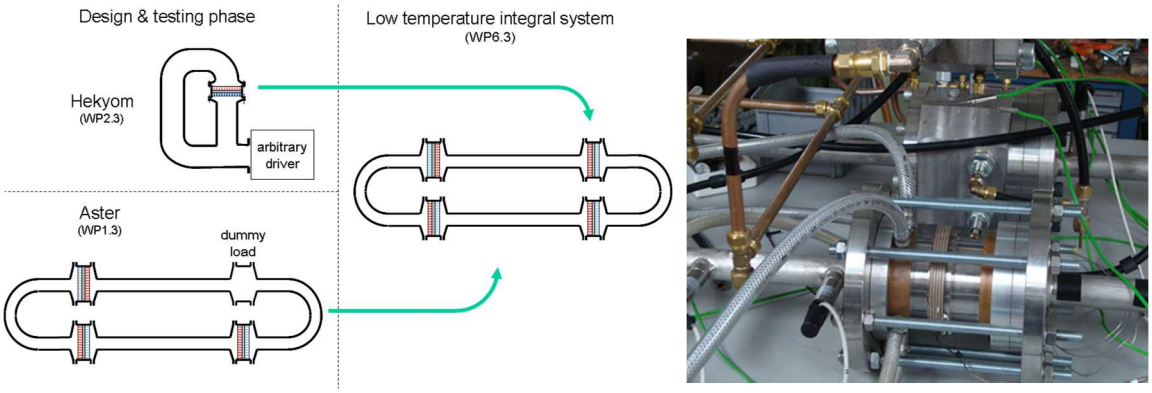

Figure 46 *Integration strategy for the low temperature system*

Figure 47 gives both the measured ΔP_{ac_loop} / ΔT curve for the initial 4 stage engine and the 3-stage engine loaded with the refrigerator (zero temperature lift).

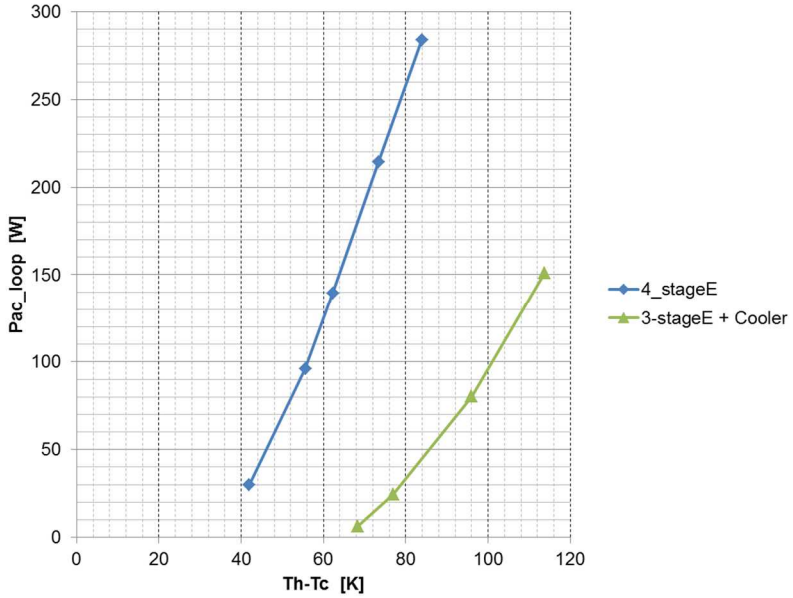

Figure 47 *The ΔPac_loop / ΔT curve for the initial 4 stage engine and the 3-stage engine loaded with the refrigerator cell (zero temperature lift) as a function of the input temperature difference*

Surprisingly there is hardly any streaming observed in this geometry. This can be partially explained by the fact that for the same acoustic loop power in a traveling wave feedback loop the amplitude is nearly half the amplitude in a standing wave resonator. Knowing that streaming is proportional with pressure amplitude this account for halving the streaming. The remaining lack of streaming however is not understood yet but fortunately it is found to be reproducible. Absence of streaming is also observed in other similar but even much larger multistage traveling wave feedback systems.

The performance of the low temperature integral system is measured at three different engine input temperatures, yielding three different drive ratio's at the refrigerator. Table 8 shows a summary of the engine and refrigerator performance.

Table 8 *Performance of the WP6 integrated system measured at increasing engine input temperature*

Engine					
T_{H_E}	Hot hex input temperature	ºC	169	211	239
T_{H_reg}	Regenerator high temperature	ºC	138	178	199
T_{C_reg}	Regenerator low temperature	ºC	32.1	38.8	47
η_{T_E}	Thermal efficiency (W_{out_E} / Q_E)	-	0.10	0.14	0.15
η_{2_E}	Exegetic efficiency relative to T_{H_E}	-	**0.29**	**0.34**	**0.35**
Refrigerator					
dr	Drive ratio at cold hex	%	1.33	1.53	1.78
T_{c_R}	Cold hex temperature	ºC	-33.7	-40.5	-45.5
COP	(Q_{C_R} / W_{in_R})	-	1.42	1.02	0.67
η_{2_R}	Exegetic efficiency relative to T_{C_R}	-	**0.32**	**0.29**	**0.19**

Table 9 presents the original the targets for the overall performance including engine, refrigerator and acoustic feedback or resonance circuit with the realized values.

Table 9 *Target and realized overall performance of the low temperature integrated system*

	Project plan	Realized
Exergetic efficiency engine	0.40	0.34
Exergetic efficiency refrigerator	0.40	0.29
Resonator efficiency	0.90	0.84
Overall exergetic efficiency	**0.140**	**0.084**

Conclusions

The realized overall performance of the low temperature integral system does not fully meet the target value specified in the project plan defined as the product of the exergetic efficiencies of the individual system parts. Causes of this deviation are identified and are found to be a consequence of engineering and chosen implementations, rather than be fundamental in nature.

Main cause of not reaching the engine efficiency is the high temperature drop across the low cost heat exchangers used in the engine stages. This temperature drop cause the engine running effectively on a 50°C lower temperature as was applied from the heat source.

Main cause of not reaching the cooler efficiency is declining of the regenerator impedance at increasing pressure amplitude or drive ratio. In the current setup it was not possible to compensate for that for practical reasons. Compensating for this effect requires slightly different lengths of the feedback tubes which was not feasible in the folded construction.

This all has paved the way towards realistic applications in the field of waste heat recovery, solar powered cooling gas liquefaction and more. Based on this geometry commercial development for some applications is already started.

Summarizing, the multi-stage traveling wave geometry proposed and developed for the WP6 low temperature integrated system has proven to be successful in reaching a low engine onset and operating temperature and in system compactness because of the internal gas volume is less than a quarter of the internal volume of the standing wave-torus geometry. It has also proven that a thermoacoustic refrigerator cell inserted into this traveling wave geometry could performance similar as in existing torus or bypass configurations.

4. Potential impact and the main dissemination activities and exploitation of results

4.1 Exploitation and impact

Thermoacoustic knowledge and in particular the knowledge obtained from THATEA can be exploited in several ways. A large number of product-market combinations can be realized with thermoacoustics, as already stated in the project proposal. As a general overview the next table is presented. The horizontal axis describes the different ways a thermoacoustic system can be driven. The vertical axis presents the different 'products'. On the horizontal axis, a difference is made in low-temperature heat (waste heat, solar heat), high-temperature heat (burner, electrical heater) and a linear motor (electrically driven). The products are heat, cold, and power (electricity, work). Multiple products can be combined into one system. A heat/heat product refers to a system that produces heat at two (or more) temperature levels. An 'X" denotes a combination that make very little sense from an energy point of view.

Drive Product	Waste heat $T_h < 200ºC$	Solar heat $T_h < 200ºC$	Burner Electrical heater	Linear motor
Process heat	Process industry	Developing countries Small-scale processes	Process industry Dwellings Offices	Process industry Dwellings Offices
Cold	Process industry Transportation	Developing countries Air-conditioning Refrigerator/freezer	Liquefaction Refrigerator/freezer	Liquefaction Refrigerator/freezer Transportation
Power	Geothermal Transportation Process industry	Photovoltaic (PV) market	Small-scale electricity production	X
Heat/cold	Food industry		Food industry	Food industry
Heat/power	Dwellings Offices Process industry	PV-Thermal market	Dwellings Offices Process industry	X
Heat/heat	Process industry	Developing countries Small-scale processes	Process industry	X

As illustrated above, the list of possible applications is very wide since thermoacoustic energy conversion can be applied as a very general energy technology involving engines and heat pumps. This is truly generic technology which application crosses all sectors. Since the operating principle and the technology base is the same for each of these applications, this offers great benefits to the economic feasibility. Application development for a specific situation in a specific sector can take advantage of similar developments taking place for a different application, both technically and economically. Whether a development leads to success depends on a number of criteria which differ per application. A general list of the criteria that are relevant for success is given here.

- Operating conditions. Do the conditions of the application match with the conditions under which a TA-system can be applied?
- Environmental and safety aspects. Does the TA-system pose any environmental or safety concerns? Since these systems generally use Helium as working medium, environmental aspects should be of no concern. Safety aspects can be relevant since TA-systems are pressure vessels.
- Integration aspects. Can the TA-system easily be integrated into the existing system or is it only applicable in new designs?
- Performance. What is the efficiency of the TA-system? This efficiency is defined as the useful product (heat, cold, electricity) divided by the required input (heat, natural gas, electricity).
- Reliability & Maintenance. What is the reliability of the system and in relation to this, what are the maintenance requirements? In general, TA-systems are considered very reliable.

- Control & start-up. Is the system easy to control and start-up?
- Acceptance. What is the acceptance of the targeted end-user for TA-technology?
- Maximum System size (power/capacity). Can the system be scaled up sufficiently to meet the desired scale level?
- Size. Are their geometrical constraints that limit the application of TA-systems?
- System Cost. What are the system costs, including integration into the application?

This project had a large focus on efficiency. The project demonstrated that the required efficiencies can be met on a component level but additional work is still needed to achieve this at a system level. The following applications are pursued by one or more partners for further development and commercialization.

Industrial waste heat transformer
A thermoacoustic waste heat transformer consists of a waste heat driven thermoacoustic engine coupled with a heat pump. The engine runs between the temperature of industrial waste heat and ambient temperature. The acoustic power that is generated from this engine is used in a heat pump that upgrades heat from waste heat to process heat levels. This concept need sufficiently high temperatures to drive the engine. Therefore this concept is specifically applicable where waste heat temperature are relatively high. In addition, the process heat level should be in the order of 50-100°C higher than the waste heat. The main target sector for this application is the (petro)chemical and refining sector. Key success factors are efficiency, costs, and whether the system can be scaled to industrial power levels. Targeted efficiency is 20-25% (process heat out/waste heat in). Targeted power per system is 1 MW waste heat. The waste heat potential within Europe is estimated at 26 EJ. Even if only one quarter is available and the efficiency of the thermoacoustic system is 25% (which is feasible based on the targeted objectives), 6.5 EJ of waste heat can be upgraded to 1.6 EJ useful heat. ECN works on this concept in cooperation with two Dutch equipment manufacturers.

Industrial linear motor driven heat pump
This system consists of an electrically driven linear motor which produces acoustic power for a heat pump. A thermoacoustic heat pump is very flexible with respect to operating temperature and required temperature lift. The heat pump will upgrade waste heat to usable temperature levels. In particular this system can be used in combination with distillation columns present in the (petro)chemical industry. The fluids in these columns are boiled by, for example, steam of 150°C. The vapor in the column is condensed at 100°C. A heat pump can upgrade the condensation heat to provide heat for the boiling process. Conventional heat pumps are not able to provide this function in an economical way. Key success factors are efficiency, costs, and whether the system can be scaled to industrial power levels. The estimated saving potential within Europe is 0.2 EJ. ECN works on this system in cooperation with major chemical companies.

High-temperature driven heat pump for industrial and domestic/office applications
An interesting application for both industry and build environment is to use a high-temperature engine (burner driven) coupled to a heat pump. For the build environment, the heat pump would operate between 10°C and 60-80°C as studied within this project. For industrial applications, a wide variety of temperatures could applied. The knowledge obtained from the THATEA project can be used to develop applications in this area. Key success factors depend on the application. For industrial purposes, costs, efficiency, integration, and scalability will be an issue. In the build environment, energy prices are higher and permitted payback times longer, therefore requirements can be less strict with respect to efficiency and costs. Size will be an important issue here. If the targeted performances on a system level can be reached, the estimated energy savings for domestic applications is about 1 EJ for Europe. The industrial savings are very hard to estimate since this depends on the specific situation and needs to be evaluated on a case by case basis. ECN is pursuing this application.

CNRS
In general the knowledge gained by THATEA will be used for academic research purposes within CNRS. This holds specifically for the work on heat exchangers and streaming phenomena. The more application oriented work is done in cooperation with Hekyom, specifically on solar driven cooling. CNRS cooperates with Hekyom on this development. A more extensive description is found below at the activities of Hekyom.

Thermoacoustic power production
A pilot is built of a multi-stage thermoacoustic power generator at an industrial plant to convert 100 kW waste heat at 160ºC into 10 kW electricity. Aim of this pilot is to demonstrate thermoacoustics on an industrial scale and the integration into an existing production process. This activity is carried out in the SBIR frame work by Aster together with two Dutch companies, Innoforte (www.innoforte.nl/) en Huisman Innovations (www.huisman-elektro.nl/innovations/) . After successful completion of the pilot the thermal and electric power levels will be scaled up first to become economic viable. Because of the pilot is not completed yet, market introduction by the commercial partner(s) is expect to start now in 2014.

Solar cooling
A prototype of a solar heat powered cooler is under construction by Aster as an add-on for vacuum tube based solar collector systems. This activity is carried out in collaboration with Watt, a Polish solar collector manufacturer (www.watt.pl/en/) and Thermo Acoustic Solutions (TAS) a Polish research/investment company.

Gas liquefaction
The market for gas liquefaction is expanding rapidly. Because of the extreme temperature range of thermoacoustic cooling it could become an important technology in this field. Together with Frames, a gas processing company (www.frames-group.com/), the feasibility of this technology for liquefying bio-gas is under investigation by Aster.

Small scale electricity generation for rural area
The UK based Score project (www.score.uk.com/) aims to develop a wood burning stove that generates electricity and refrigeration for rural areas and developing countries. The multi-stage concept is introduced in the project and small scale (local) production of those stoves equipped with a 2-stage thermoacoustic engine is foreseen in 2013.

Industrial refrigeration
A thermoacoustic chiller is under development at HEKYOM. Its aim is to cool an industrial refrigerated cabinet and pump 350 Watt at – 15°C. For compactness and efficiency, a linear alternator is used to generate the acoustic wave needed by the thermoacoustic loop refrigerator. Such a project, made with a French company and supported by ADEME, is in progress.

Solar driven cooling
A promising concept is to use thermoacoustic technology to convert solar heat directly into cooling. Thermoacoustic is indeed currently the only device that can accept such high temperature level, allowing higher efficiency compared to adsorption or absorption systems. HEKYOM is involved in such a program with CNRS, supported par the French national Research Agency.

Waste heat or Solar heat to electricity
HEKYOM is involved into several industrial projects in which the energy source would be waste heat like exhaust gas of thermal engine, fumes or solar energy. The goal is to generate about 1 to 5 kilowatts of electricity. HEKYOM has made a patent deposit demand in 2010 and 2011 with a PCT procedure in 2011. He has also ordered an economic promotion and development of such a machine: “heat to electricity” from a patent Company in 2010 and 2011.

4.2 Dissemination

This section contains an overview of the peer reviewed publications and the other dissemination activities with respect to the THATEA project.

Peer reviewed publications

Shi L, Yu Z and Jaworski AJ 2011 Investigation into the Strouhal numbers associated with vortex shedding from parallel-plate thermoacoustic stacks in oscillatory flow conditions, to *European Journal of Mechanics – B/Fluids*, **30**(2), 206-217.

Abduljalil ARS, Yu Z and Jaworski AJ 2011 Selection and experimental evaluation of low-cost porous materials for regenerator applications in thermoacoustic engines, *Materials and Design*, **32**(1), 217-228.

Shi L, Mao X and Jaworski AJ 2010 Application of planar laser induced fluorescence measurement techniques to study heat transfer characteristics of parallel-plate heat exchangers in thermoacoustic devices, *Measurement Science and Technology*, **21**(11), 115405 (16pp).

Blok. C.A.M. de, *Novel 4-stage travelling-wave thermoacoustic power generator*, Proceedings ASME-FEDSM-ICNMM2010, Montreal, Canada, 1-5 August 2010.

Vanapalli S., Tijani M.E.H., Spoelstra S., *Thermoacoustic-stirling heat pump for domestic applications,* Proceedings ASME-FEDSM-ICNMM2010, Montreal, Canada, 1-5 August 2010.

Tijani, M.E.H., Vanapalli, S., Spoelstra, S., *Design of a mechanical resonator to be coupled to a thermoacoustic stirling-engine*, Proceedings ASME-FEDSM-ICNMM2010, Montreal, Canada, 1-5 August 2010.

Piccolo, A., *Heat transfer characteristics of parallel plate thermoacoustic heat exchangers,* Proceedings of the ASME-ATI-UIT 2010 Conference Thermal and Environmental Issues in Energy Systems, 16-19 May 2010, Pisa, Italy

Piccolo, A., La Face, L., Ponterio, L., *Entropy generation characteristics of thermoacoustic stacks and heat exchangers*, Proceedings of Thrid International Conference on Applied Energy, May 16-18 2011, Perugia, Italy.

Pierens, M., *Experimental characterization of a thermoacoustic travelling-wave refrigerator*, Proceedings of the International Conference on Fluid Mechanics, Heat Transfer and Thermodynamics, July 13-15 2011, Amsterdam, the Netherlands.

Piccolo, A., *Numerical computation for parallel plate thermoacoustic heat exchangers in standing wave oscillatory flow,* International Journal of Heat and Mass Transfer, 2011 Vol 54, 4518-4530.

Piccolo, A., Jaworski, A.J., Mao, X., *Experimental and numerical study of temperature distribution and heat transfer in parallel-plate thermoacoustic heat exchangers,* Proceedings 66th National Congress of Associazione Termotecnica Italiana (ATI), 5-9 September 2011, Italy.

Yu, Z., *Experimental testing of the flow resistance and thermal conductivity of porous materials for regenerators,* Proceedings 23rd IIR International Congress of Refrigeration, 21-26 August 2011, Prague.

Saat, F.A.Z., Yu, Z., Jaworski, A.J.,*CFD-assisted regenerator analysis: application to thermoacoustic system*, Proceedings 23rd IIR International Congress of Refrigeration, 21-26 August 2011, Prague.

Mao, X., Kamsanam, W., Jaworski, A.J*., Convective heat transfer from fins-on-tubes heat exchangers in an oscillatory flow,* Proceedings 23rd IIR International Congress of Refrigeration, 21-26 August 2011, Prague.

Mao, X., Shi, L., Jaworski, A.J., Kamsanam, W., *Heat Transfer on Parallel Plate Heat Exchangers in an Oscillatory Flow,* Proceedings 10th Biennial Conference on Engineering Systems Design and Analysis, 12-14 July 2010, Istanbul

Piccolo, A., *Impact of heat exchanger fin length and spacing on the cooling power of standing wave thermoacoustic refrigerator,* Proceedings 66th National Congress of Associazione Termotecnica Italiana (ATI), 5-9 September 2011, Italy.

Dissemination activities

Type of activity	Partner	Title	Date & Place	Audience
Presentation at Conference	UNIME	66th National Congress of Associazione Termotecnica Italiana (ATI),	5-9 September 2011, Calabria	Scientific community
Presentations at Conference	UNIMAN	23rd IIR International Congress of Refrigeration	21-26 August 2011, Prague	Scientific community Industry
Presentation at Conference	UNIMAN	10th Biennial Conference on Engineering Systems Design and Analysis	12-14 July 2010, Istanbul	Scientific community
Presentations at Conference	ECN Aster	ASME 3rd Joint US-European Fluids Engineering Summer Meeting	1-5 August 2010, Montreal	Scientific community Industry
Presentation	Aster	Thermo Acoustic Power (TAP)	23 March 2011, Utrecht	Industry
Presentation	Aster	Border crossing acoustics	23 November 2011, Utrecht	Scientific community
Presentation	Aster	Introduction to thermoacoustics	14 December 2009, Wroclaw	Scientific community Students
Presentations at Conference	ECN Aster	The 19th international Congres on Sound and vibration	8-12 July 2012, Vilnius	Scientific community
Presentations at workshop	CNRS ECN	Journee Thermoacoustique SFT/SFA	10 December 2010, Paris	Scientific community Industry
Presentations at Conference	Aster	International Conference on "Low-cost, electricity generating heat engines for rural areas	2-3 April 2012, Nottingham	Civil society
Presentation at Conference	ECN	Acoustics 2012	1-5 August 2012, Nantes	Scientific community Industry
Presentation at Conference	ECN	Heat Powered Cycles Conference Co-organised by ECN	10-12 September 2012, Alkmaar	Scientific community Industry
Presentation at Conference	CNRS	International Conference on Fluid Mechanics, heat transfer and Thermodynamics	13 July 2011, Amsterdam	Scientific community
Contribution to festival	CNRS	Fete de la science	16 October 2011, Orsay	Civil society
Interview	Hekyom	Thermoacoustics: Process and industrial applications	4 February 2010	Scientific community Industry Civil society
Contribution to festival	UNIME	Festival dell'Energia (Festival of Energy)	15 June 2012, Perugia	Industry Civil society Policy makers
Thesis	UNIME	Computational thermofluiddynamics for the study of thermoacoustic systems	2012	Scientific community
Articles in popular press	ECN	Projects Magazine - Thermoacoustics, the dawn of a new era in energy production?	March 2012	Civil society Policy makers

5. Contact details

Project website www.thatea.eu

Partners and contact persons

Partner	Contact person	E-mail address	Phone number
ECN	S. Spoelstra	spoelstra@ecn.nl	+31 224564523
CNRS	J.P. Thermeau	thermeau@ipno.in2p3.fr	+33 169157902
UNIMAN	A.J. Jaworski	aj160@leicester.ac.uk	+44 1162231033
Aster	C.M. de Blok	info@aster-thermoacoustics.com	+31 578631103
UNIME	A. Piccolo	apiccolo@unime.it	+39 0903977311
Hekyom	T. le Polles	thierry.lepolles@hekyom.com	+33 673356090
NRG	M. Loginov	loginov@nrg.eu	+31 224568191